

Novel non-canonical strigolactone analogs highlight selectivity for stimulating germination in two Phelipanche ramosa populations

Suzanne Daignan Fornier, Alexandre de Saint Germain, Pascal Retailleau, Jean-Paul Pillot, Quentin Taulera, Lucile Andna, Laurence Miesch, Soizic Rochange, Jean-Bernard Pouvreau, François-Didier Boyer

▶ **To cite this version:**

Suzanne Daignan Fornier, Alexandre de Saint Germain, Pascal Retailleau, Jean-Paul Pillot, Quentin Taulera, et al.. Novel non-canonical strigolactone analogs highlight selectivity for stimulating germination in two Phelipanche ramosa populations. 2022. hal-03616875

HAL Id: hal-03616875
https://hal.science/hal-03616875

Preprint submitted on 23 Mar 2022

HAL is a multi-disciplinary open access archive for the deposit and dissemination of scientific research documents, whether they are published or not. The documents may come from teaching and research institutions in France or abroad, or from public or private research centers.

L'archive ouverte pluridisciplinaire **HAL**, est destinée au dépôt et à la diffusion de documents scientifiques de niveau recherche, publiés ou non, émanant des établissements d'enseignement et de recherche français ou étrangers, des laboratoires publics ou privés.

Novel non-canonical strigolactone analogs highlight selectivity for stimulating germination in two *Phelipanche ramosa* populations

Suzanne Daignan Fornier[1], Alexandre de Saint Germain[2], Pascal Retailleau[1], Jean-Paul Pillot[2], Quentin Taulera[3], Lucile Andna[4], Laurence Miesch[4], Soizic Rochange[3], Jean-Bernard Pouvreau[5], François-Didier Boyer[1*]

[1] Université Paris-Saclay, CNRS, Institut de Chimie des Substances Naturelles, UPR 2301, 91198, Gif-sur-Yvette, France

[2] Université Paris-Saclay, INRAE, AgroParisTech, Institut Jean-Pierre Bourgin (IJPB), 78000, Versailles, France

[3] Laboratoire de Recherche en Sciences Végétales, Université de Toulouse, CNRS, UPS, Toulouse INP, 31320 Auzeville-Tolosane, France

[4] Université de Strasbourg, Institut de Chimie, UMR 7177, Équipe Synthèse Organique et Phytochimie, 4 rue Blaise Pascal CS 90032, 67081 Strasbourg Cedex, France

[5] Nantes Université, CNRS, US2BN, UMR 6286, F-44000 Nantes, France

KEY WORDS: *Phelipanche ramosa, Parasitic weeds, Germination stimulants, Strigolactones, Synthetic analogs, Structure-activity relationship, Plant hormone, Pisum sativum, Arabidopsis thaliana, Rhizophagus irregularis.*

ABSTRACT: Strigolactones (SLs) are plant hormones exuded in the rhizosphere with a signaling role for the development of arbuscular mycorrhizal (AM) fungi and as stimulants of seed germination of the parasitic weeds *Orobanche*, *Phelipanche* and *Striga*, the most threatening weeds of major crops worldwide. *Phelipanche ramosa* is present mainly on rape, hemp and tobacco. *P. ramosa* 2a preferentially attacks hemp while *P. ramosa* 1 attacks rapeseed. The recently isolated Cannalactone **14** from hemp root exudates has been characterized as a non-canonical SL that selectively stimulates the germination of *P. ramosa* 2a seeds in comparison with *P. ramosa* 1. In the present work, we established that (–)-solanacol **5**, a canonical orobanchol-type SL exuded by tobacco and tomato, possesses a remarkable selective germination stimulant activity for *P. ramosa* 2a seeds**.** We synthesized cannalactone analogs, named (±)-SdL19 and (±)-SdL118 which have an unsaturated acyclic carbon chain with a tertiary hydroxyl group and a methyl or a cyclopropyl group instead of a cyclohexane A-ring, respectively. (±)-SdL analogs are able to selectively stimulate *P. ramosa* 2a revealing that these minimal structural elements are key for this selective bioactivity. In addition, we showed that (±)-SdL19 is able to inhibit shoot branching in *Pisum sativum* and *Arabidopsis thaliana*, and induces hyphal branching in AM fungus *R. irregularis*, like SLs.

INTRODUCTION

Strigolactones (SLs) are a class of compounds first identified in 1966[1] as stimulants of seed germination of the root parasitic weeds *Orobanche*, *Phelipanche* and *Striga*. More recently, SLs have been discovered as the 9th class of plant hormone that control plant architecture including shoot branching stem secondary growth, plant height, root architecture, and adventitious roots[2-5]. They are synthesized in plant roots in trace concentrations, and are partly excreted into the rhizosphere. They belong to the apocarotenoid family (Scheme 1). The structural core of SLs is a tricyclic lactone (ABC part, canonical SLs) or an unclosed BC-ring (non-canonical SLs) connected via an enol ether bridge to an invariant α,β-unsaturated furanone moiety (D ring). All natural SLs have the same *R*-configuration at the C-2' position. Canonical SLs are divided into strigol (**1**) and orobanchol (**2**) -types corresponding to a β- (e.g., 5-deoxystrigol **4**, sorgolactone **7**) or an α-oriented C-ring (e.g., orobanchyl acetate **3**, solanacol **5**, solanacyl acetate **6**, fabacyl acetate **8**), respectively and with A and B cycles bearing various substituents (Chart 1**A**)[6]. Non-canonical SLs (e.g., avenaol **11**, zealactone **12**, bryosymbiol **13** and cannalactone **14**) can be structurally more diverse than canonical SLs (Chart 1**B**). The common biosynthetic precursors for canonical and non-canonical SLs are carlactonoic acid **18** (CLA) and hydroxy-carlactonoic acids (HO-CLAs)[7-9] biosynthesized from all-*trans*-β-carotene **17** via carlactone **9** (CL) and hydroxy-carlactones (HO-CLs) (Scheme 1)[10,11]. In addition, methyl carlactonoate (MeCLA **10**) and HO-MeCLAs[12,13] have been identified as biosynthetic precursors for numerous non-canonical SLs.

To date, more than 23 canonical SLs and more than 10 non-canonical SLs have been identified in plant root exudates and plant tissues[14]. Natural SLs are difficult to obtain by organic synthesis due to long multistep syntheses[15-18]. Numerous SL analogs and mimics have been developed for plant chemical biology[19,20]. GR24, invented by **G**erald **R**osbery, is a canonical strigol-type SL analog with an aromatic A-ring[21]. GR24, in most cases as racemic mixture, is the worldwide reference compound (Chart 1**C**) in all assays investigating the role of SL in biological processes. The simplified GR-type compound GR5[21], possessing only C and D rings (Chart 1**C**) has been also developed as a germination stimulant of root parasitic plant seeds and proved later to

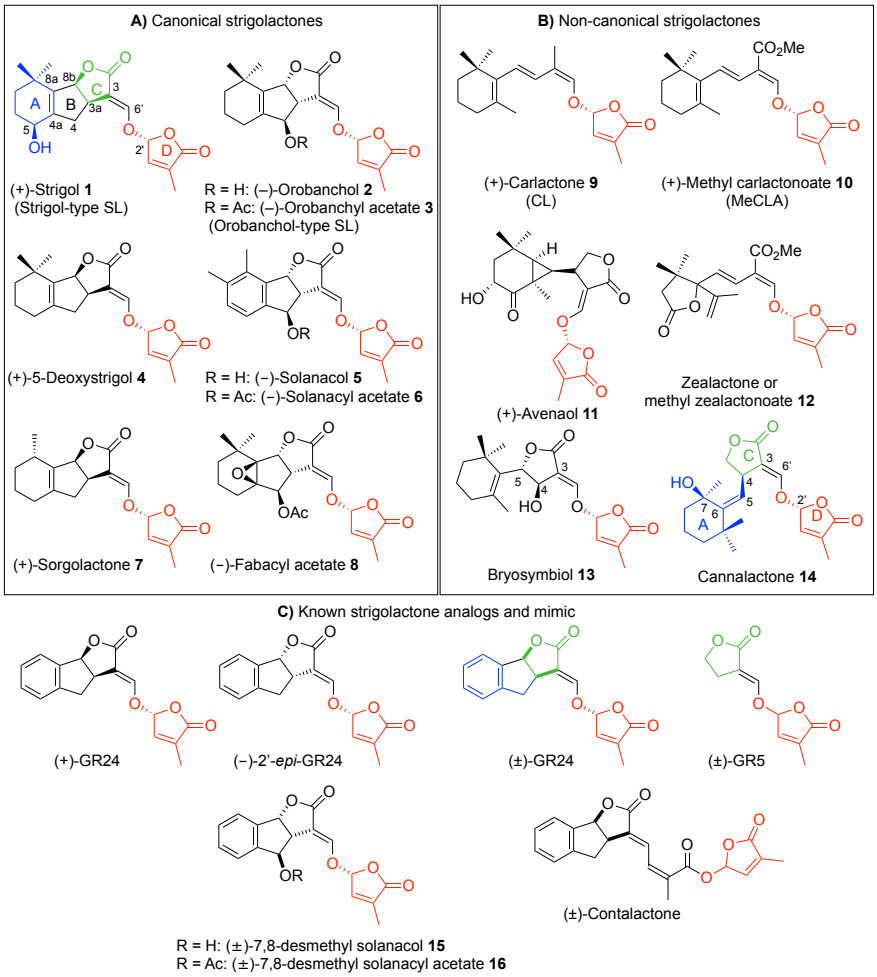
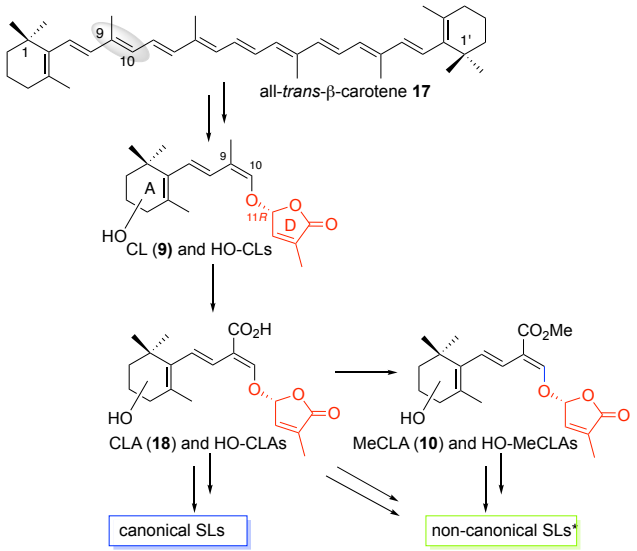


Chart 1. Natural strigolactones (SLs), canonical (A), non-canonical (B) and artificial SL analogs and mimic (C). For bryosymbiol, the absolute stereochemistry at C-4 and C-5 could be interchangeable[22].



Scheme 1. Strigolactone biosynthetic scheme. CL= carlactone ; CLA = carlactonoic acid ; MeCLA = methyl carlactonoate ; SL strigolactone. * Isolated and identified to date.

be bioactive as plant hormone in the control of shoot branching[23-25]. More recently, CL[26] and MeCLA non-canonical SL synthetic analogs[27,28] have been developed to study the bioactivity of structures close to highly unstable CL **9** and MeCLA **10**[14].

The parasitic plants *Orobanche, Phelipanche* and *Striga* are major agricultural pests around the Mediterranean Sea and in Sub-Saharan Africa, respectively. They tragically constitute there a major cause of crop damage[29] in intensive crop systems that is expected to expand to new territories in the near future[30]. They are obligate parasites producing numerous and extremely small seeds that can remain viable in soil for decades before germination[31].

The induction of germination by host plant SLs is a critical step in the development cycle of these weeds[32]. SL synthesis and signaling are therefore important targets for crop protection[20,33].

SLs have been shown to play an additional rhizospheric signaling role by stimulating spore germination and hyphal proliferation of AM fungi[34,35]. The hypothesis is that plant SLs boost fungal metabolism prior to root infection[36]. The AM symbiosis arose very early in land plant evolution and is thought to have been instrumental in allowing successful plant conquest of terrestrial environments[37]. It has been proposed that an ancestral role of SLs was to attract these highly beneficial fungal symbionts[22], root parasitic plants having highjacked this system much later to detect their host[25]. Biological activities of SLs could be detected at concentrations as low as 10^{-13} M on AM fungi, 10^{-12} M on seeds of parasitic weeds and 10^{-8} M on lateral buds as plant hormone.

Phelipanche ramosa seeds recognize allelochemical signals and interact with their hosts depending on their genetic structure as reported recently[38,39]. Three main genotypic groups were described in European *P. ramosa* populations from the Mediterranean basin. *P. ramosa* of genetic group 1 (*P. ramosa* 1) is present exclusively in western France. It parasites essentially oilseed rape but also melon, tobacco, and sunflower. *P. ramosa* 2a attacks preferentially hemp but also tobacco and tomato in France and Italy. *P. ramosa* 2b is widespread in in Europe and Turkey and attacks mainly tobacco but also various crops like oilseed rape, hemp and tomato. Seed sensitivity to germination stimulants as SLs emitted by host plants is proposed as marker of genetic groups. In oilseed rape no SL has been yet identified[40]. Tobacco plants exude canonical strigol-type and orobanchol-type SLs[41,42] and tomato plants exude orobanchol-type SLs[43]. The non-canonical SL cannalactone **14** has been recently characterized from hemp (*Cannabis sativa*)[44]. Differential sensitivities to synthetic GR24 enantiomers and cannalactone **14** for germination of *P. ramosa* seeds of different genetic groups have been reported[39,44,45].

The SL receptor in vascular plants DWARF14 (D14) has been identified as a member of the superfamily of the α/β-hydrolases[4,46]. In *Arabidopsis*, a paralog of AtD14, KARRIKIN INSENSITIVE2/HYPOSENSITIVE TO LIGHT (AtKAI2 /AtHTL), has also been described. It encodes a protein that shows a global structure very similar to AtD14 and has conserved the catalytic triad (Ser, His, Asp). AtKAI2 has been shown to regulate *Arabidopsis* seed germination[47]. Interestingly, the *KAI2* gene family has expanded during the evolution of parasitic plant genomes. Some members of these expanded families in witchweeds and broomrapes have evolved the capacity to bind SLs, making them good candidates for SL receptors. Six of the 11 *S. hermonthica* KAI2 paralogs, belonging to the divergent clade, were identified as highly sensitive to SLs[48-50]. These results indicated the involvment of one or several α/β-hydrolases in SL perception in parasitic plants. In *P. ramosa* 1, among the 5 KAI2 paralogs, we recently established that PrKAI2d3 encodes a SL receptor which is also able to interact with isothiocyanates (ITCs), other germination stimulants of *P. ramosa* seeds[51].

The objective of the present work is to analyze the biological activity of various cannalactone analogs in comparison with natural cannalactone **14**, natural SLs and especially SLs produced by tobacco[41,42] and tomato[43] ((–)-orobanchol **2,** (–)-orobanchyl acetate **3**, 5-deoxystrigol **4**, (–)-solanacol **5** and (–)-solanacyl acetate **6**), the SL mimic contalactone[45] and well-known GR SL analogs. Through a structure-activity relationship (SAR) study, we decipher key minimal structural elements for selective germination activity of *P. ramosa* seeds focused on *P. ramosa* 1 *versus* 2a[38] which attack selectively major crops as rapeseed and hemp, respectively. Moreover, we show that these novel non-canonical SL analogs possess hormonal activity in pea and induce hyphal branching in arbuscular mycorrhizal (AM) fungi.

RESULT AND DISCUSSION

Synthesis of cannalactone analogs. We designed two types of cannalactone analogs (Chart 2). Type I possesses an unsaturated acyclic chain instead of the cyclohexane A-ring of cannalactone **14**. Type II bears an unsaturated acyclic carbon chain with a tertiary hydroxyl group and a methyl or a cyclopropyl group (R^2 group) replacing the cyclohexane A-ring.

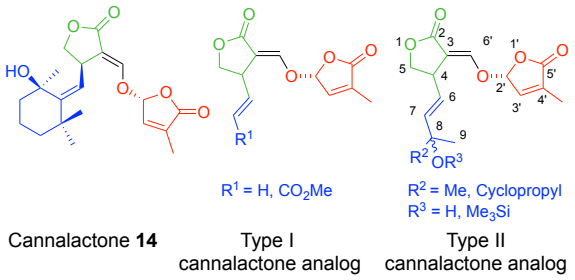
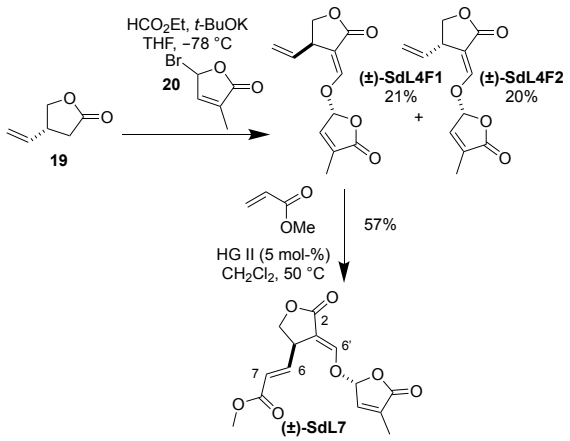


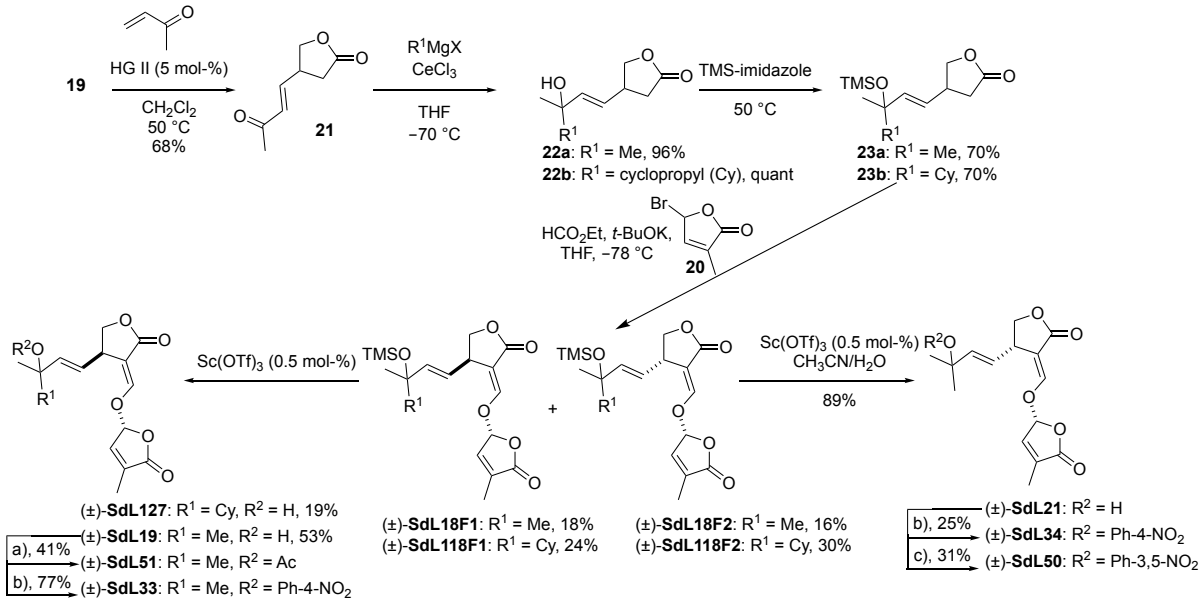
Chart 2. Cannalactone analogs Type I and II designed in this work. Numbering for cannalactone analogs (SdL) and chemicals synthesized here.

The starting material for type I and type II analogs is (±)-4-vinyldihydrofuran-2(*3H*)-one **19** or Taniguchi lactone[52] prepared at multigram-scale from the commercially available *cis*-2-butene-1,4-diol via formation of a ketene acetal and its [3,3]-sigmatropic rearrangement. Formylation of (±)-Taniguchi lactone and one-pot coupling with D-Br **20** at −78 °C led to the formation of diastereomers Type-I cannalactone analogs (±)-SdL4F1 and (±)-SdL4F2 easily separable by silica gel chromatography in 41% overall yield (Scheme 2). SdL7, another Type-I cannalactone analog was obtained by cross metathesis (CM) of (±)-SdL4F1 with a large excess of methyl acrylate at 50 °C with Hoveyda-Grubbs II (HG II) initiator in 57% yield. The *E*-geometry of the α,β-unsaturated ester group and the *E*-geometry of the enol function in SdL7 were proven by NMR analysis ($^3J_{H6\text{-}H7}$ = 15.5 Hz, $^3J_{C2\text{-}H6'}$ = 2.0 Hz).



Scheme 2. Preparation of Type-I cannalactone analogs: (±)-SdL4F1, (±)-SdL4F2 and (±)-SdL7.

Preparation of Type-II analogs with R^1 = methyl or cyclopropyl group involved the sequence detailed in Scheme 3. Taniguchi lactone **19** was engaged in CM with butane-3-one in presence of HG II and afforded enone **21** in 68% yield. The selective addition of methyl and cyclopropyl group on the ketone group of enone **21** was accomplished using Grignard reagents with cerium(III) chloride leading to alcohol **22a** and **22b** in near quantitative yields[53,54]. Cerium(III) chloride plays an important role in increasing the nucleophilicity and decreasing the basicity of the Grignard reagents. The direct formylation on alcohols **22a,b** was unsuccessful. However, silylation of alcohols **22a,b** in neat trimethylsilyl imidazole furnished protected derivatives **23a,b** in 70% yield, which led by formylation and coupling with D-Br **20** to a separable mixture of diastereomers in moderate yields (34-54%) ((±)-SdL18F1/(±)-SdL18F2**,** (±)-SdL118F1/(±)-SdL118F2). A mild deprotection of separated silylated derivatives ((±)-SdL18F1, (±)-SdL18F2) with catalytic Lewis acid ($Sc(OTf)_3$) and H_2O[55] led to both alcohols (±)-SdL19 and (±)-SdL21 in non optimized 53 and 89% yields, respectively. However, these conditions for the silylated cyclopropyl derivative (±)-SdL118F1 were inefficient but the targeted alcohol (±)-SdL127 was produced with scandium(III) triflate and Ac_2O[56] in poor 19% yield and without detection of the acetylated product. Tertiary alcohols (±)-SdL19 and (±)-SdL21 were acylated by standard conditions to furnish acetylated derivative (±)-SdL51 and 4-nitrobenzoates (±)-SdL51 and (±)-SdL50. In addition, formation of 3,5-nitrobenzoate (±)-SdL50 from (±)-SdL21 furnished a crystalline compound whose X-ray diffraction properties were sufficiently exploited to establish unambiguously the relative configurations of stereogenic centers C2' and C4 of (±)-SdL50 as 2'*R* and 4*S,* respectively (Figure 1) and by consequence the relative configurations of stereogenic centers for the other SdL analogs. With these putative SL analogs in our hands, their biological activity was studied.



Scheme 3. Preparation of Type-II cannalactone analogs (±)-SdL18F1, (±)-SdL18F2, (±)-SdL19, (±)-SdL21, (±)-SdL33, (±)-SdL34, (±)-SdL50, (±)-SdL51, (±)-SdL118 and (±)-SdL127. a) Ac_2O, 4-DMAP, pyridine, rt ; b) ClCO-Ph-4-NO_2, 4-DMAP, pyridine, 40 °C ; c) ClCO-Ph-3,5-NO_2, 4-DMAP, pyridine, 40 °C.

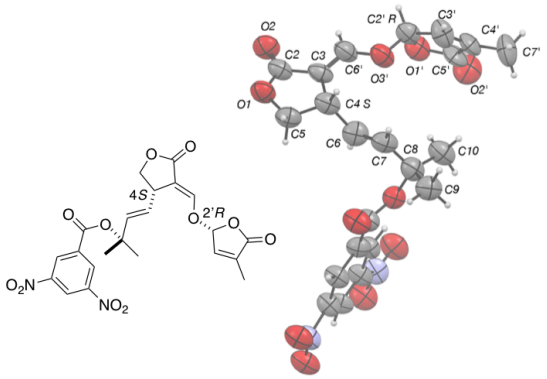


Figure 1. ORTEP view of the asymmetric unit of (±)-SdL50 (solvent molecule omitted) with selected atom numbering. Ellipsoids are represented with 30% of probability.

Most SdL derivatives possess similar bioactivity and selectivity as cannalactone toward *Phelipanche ramosa* 1 *versus* 2a. The germination stimulant activities of SdL analogs on *P. ramosa* 1 and 2a seeds were determined and compared to (±)-GR24, (±)-GR5 and natural cannalactone **14** by measuring the maximum of germination stimulant activity as well as half maximal effective concentrations (EC_{50}) using a concentration range from 10^{-13} to 10^{-6} mol.L^{-1} (Chart 3, Figure 2**A**)[57]. Germination stimulant activities of all SdL analogs and the putative cannalactone biosynthetic precursor, (±)-MeCLA, reached the maximum induced by (±)-GR24 which makes them germination stimulants as expected for SL analogues (Figure S1**A**). We compared the bioactivities of these chemicals based on EC_{50} values.

We previously reported that cannalactone **14**, a non-canonical SL, possesses a stronger germination stimulation activity on *P. ramosa* 2a than on *P. ramosa* 1. On contrary, (±)-GR24, an artificial canonical SL possesses a stronger germination stimulation activity on *P. ramosa* 1 rather than on *P. ramosa* 2a[44]. These results led us to propose that *P. ramosa* 1 could be more sensitive to canonical SLs and *P. ramosa* 2a to non-canonical SLs. To illustrate the selectivity of seed germination between *P. ramosa* 1 and *P. ramosa* 2a, the ratio of EC_{50} (*P. ramosa* 1/ *P. ramosa* 2a) (r_{EC50}) of each molecule was calculated (Figure 2**B**); for example, r_{EC50} ((±)-GR24) = 0.014 and r_{EC50} (**14**) = 410.

We studied a set of various canonical SLs belonging to strigol- ((±)-**1**, (±)-**4**, (±)-**7**) and orobanchol-types ((±)-**2**, (±)-**3**, (–)-**5**, (–)-**6**, (±)-**8**) and (±)-contalactone (Chart 1),[45] a recent SL mimic discovered during the preparation of (±)-GR24. All canonical SLs (**1-4**, **7-8**) and (±)-contalactone[45] were found less active than (±)-GR24, (+)-GR24 and (–)-2'-*epi*-GR24,[45] possessing stereochemistries found in natural canonical SLs (strigol-type and orobanchol-type, respectively). Their r_{EC50} (< 1) reflect selectivity for *P. ramosa* 1, except for the cases of (–)-solanacol **5** and (–)-solanacyl acetate **6** where high germination activity and selectivity for *P. ramosa* 2a were recorded (r_{EC50} ((–)-**5**) = 164) (Figure 3, Figure S1**B**). Though high germination activities were observed with (–)-solanacyl acetate **6** and 7,8-desmethyl solanacol derivatives **15** and **16**, selectivity was reduced, highlighting the importance of the hydroxyl group but also the methyl group on the A aromatic ring for selectivity. High levels of (–)-solanacol **5** and (–)-solanacyl acetate **6** were detected in tobacco root exudates[41] and in tomato root extracts[43]. To note, tobacco and tomato plants are also hosts for *P. ramosa* 2a[38,39], in accordance with the sensitivity of *P. ramosa* 2a seeds to (–)-solanacol **5** and (–)-solanacyl acetate **6** shown here.

We studied the germination stimulation activities of the SL biosynthetic intermediates (Scheme 1). For all-*trans*-β-carotene **17**, a SL biosynthetic precursor without D-ring, no germination was recorded, demonstrating that this compound is not bioactive and/or that no enzyme of the SL biosynthesis pathway was sufficiently present in plant parasitic seeds (Figure S1). For racemic MeCLA **10** and CL **9**, the SL biosynthetic precursors possessing the D-ring but no C ring and A ring decorated with a tertiary hydroxyl group, germination stimulation activities were drastically reduced in comparison with **14** and (±)-GR24. A small difference was observed between *P. ramosa* 1 and *P. ramosa* 2a for MeCLA **10** (r_{EC50} = 0.47), the putative biosynthetic precursor of cannalactone **14**[44] (Figure 3**B**). The specificity of biological response would appear from the compounds downstream of MeCLA in the biosynthetic pathway. Isothiocyanates (ITCs) as glucosinolate-breakdown products are germination stimulants of *P. ramosa* seeds secreted in the soil by host plants as Brassicaceae[31,40,58]. As for (±)-MeCLA **10,** a small difference of germination was observed between *P. ramosa* 1 and *P. ramosa* 2a (0.1 < r_{EC50} < 1.1 for 2-phenylethyl isothiocyanate)[39,45].

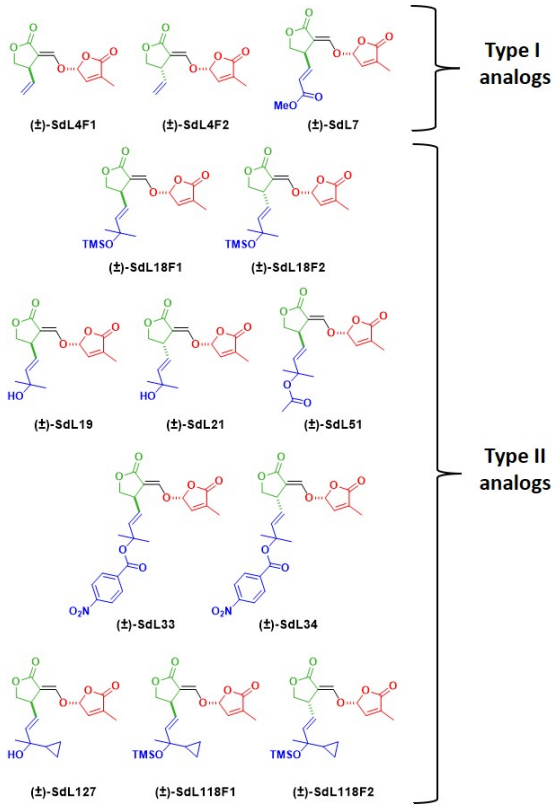


Chart 3. Cannalactone analogs synthetized for this study.

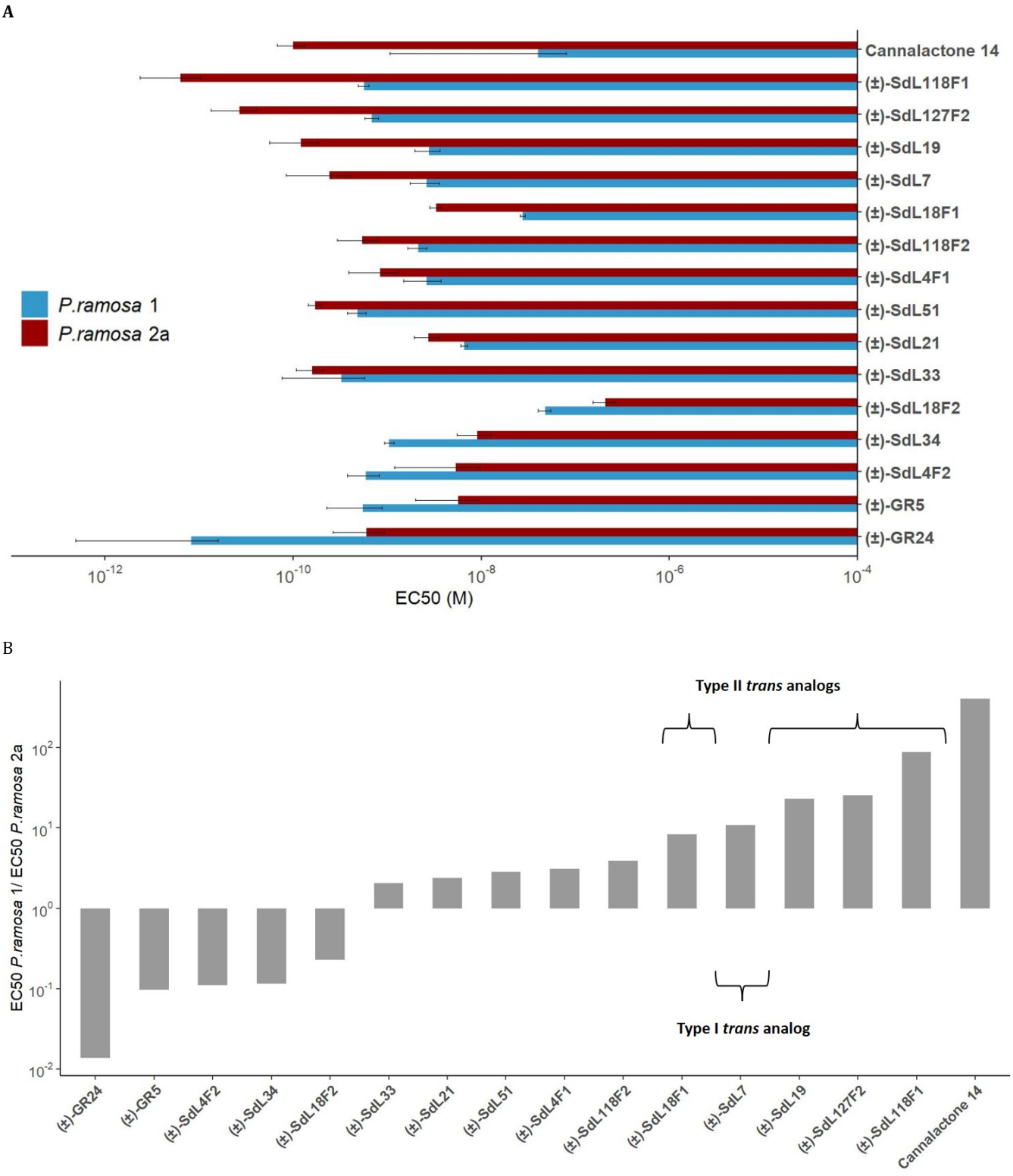


Figure 2. Bioactivity on *Phelipanche ramosa* 1 *versus Phelipanche ramosa* 2a seed germination of SdL analogs (see Chart 3). (**A**) EC_{50} (half maximal effective concentration) (mol L^{-1}) of SdL analogs, (±)-GR5, natural cannalactone **14** and (±)-GR24 toward *P. ramosa* 1 and *P. ramosa* 2a. EC_{50} are presented ± SE, ($6 \leq n \leq 12$). (**B**) r_{EC500} [EC_{50} (*P. ramosa* 1)/ EC_{50} (*P. ramosa* 2a)] for each chemical.

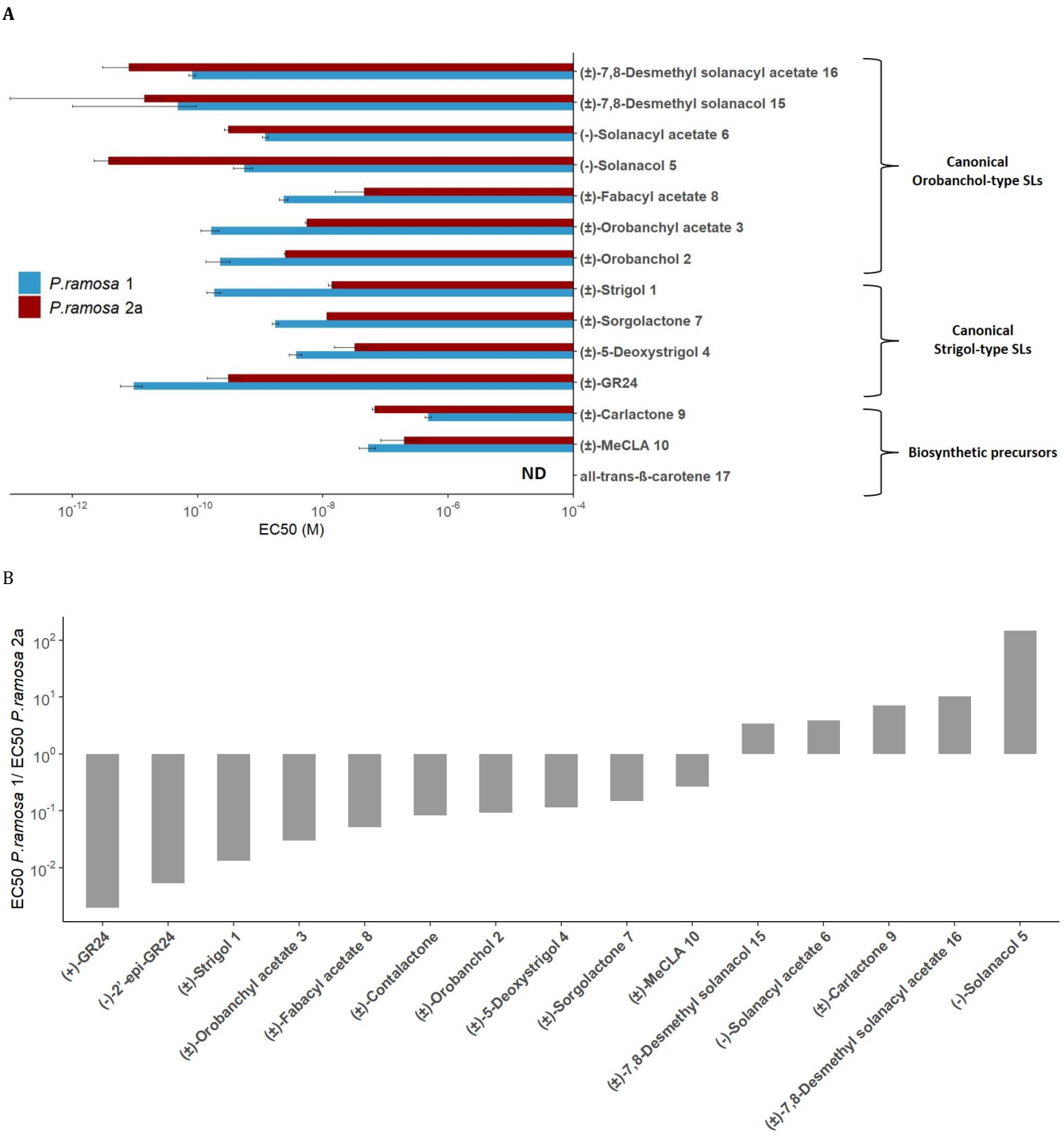


Figure 3. Bioactivity on *Phelipanche ramosa* 1 *versus Phelipanche ramosa* 2a seed germination of canonical SLs, SL biosynthetic precursors in comparison with (+)-GR24[45] and (–)-2'-*epi*-GR24[45]. (**A**) EC_{50} (half maximal effective concentration) (mol L^{-1}) of canonical SLs and (±)-GR24 toward *P. ramosa* 1 and *P. ramosa* 2a. EC_{50} are presented ± SE, ($6 \leq n \leq 12$). (**B**) r_{EC50} = EC_{50} (*P. ramosa* 1)/ EC_{50} (*P. ramosa* 2a) for each SL and (±)-contalactone[45]. ND = not determined.

Comparing the germination stimulation activities of (±)-GR5 to that of (±)-GR24, loss of cycles A and B led to bioactivity reductions but also dampened the difference between *P. ramosa* 1 and *P. ramosa* 2a (r_{EC50} ((±)-GR5) = 0.10) (Figure 2**B**). All (±)-SdL analogs are bioactive but less than (±)-GR24 for *P. ramosa* 1. (±)-SdL118F1 and (±)-SdL127F2 proved to be more bioactive toward *P. ramosa* 2a while all the other SdLs were less bioactive than cannalactone even if they have high activity for this population. SdL analogs possess EC_{50} values varying between 5.6×10^{-10}-4.8×10^{-8} M for *P. ramosa* 1, and 6.4×10^{-12}-2.1×10^{-7} M for *P. ramosa* 2a. Removal of AB rings and

replacement by an unsaturated acyclic carbon chain at C-3a position induced a loss of bioactivity toward *P. ramosa* 1 for all SdL analogs compared to (±)-GR24. Moreover, no significant difference was observed between "*cis*" (2'*R**,4*R**) and "*trans*" (2'*R**,4*S**) SdL analogs toward *P. ramosa* 1. On the other hand, on *P. ramosa* 2a seeds, SdL analogs with an acyclic unsaturated carbon chain have a bioactivity similar to (±)-GR24. For the genetic group 2a, it was also interesting to find that the (±)-*trans*-SdL analogs were more active than the (±)-*cis*-SdL analogs. It was therefore possible to classify SdL analog bioactivity using the r_{EC50} diagram (Figure 2**B**). The most active and selective molecules toward *P. ramosa* 2a are thus (±)-SdL118F1 (EC_{50}= 5.6×10^{-10} M, r_{EC50} = 87.5), (±)-SdL19 (EC_{50} = 1.5×10^{-10} M, r_{EC50} = 18.7) and (±)-SdL7 (EC_{50} = 2.4×10^{-10} M, r_{EC50} = 10.8). The analog (±)-SdL19 showed a similar selectivity for the germination of *P. ramosa* 2a *versus P. ramosa* 1 as cannalactone **14,** and a similar bioactivity toward *P. ramosa* 2a (EC_{50} 1.5×10^{-10} M *versus* 1.0×10^{-10} M) (Figure 2**A**). Subsequently, due to the ease of preparation of the compound (±)-SdL19 and its specificity, we focused on this compound in the rest of this study.

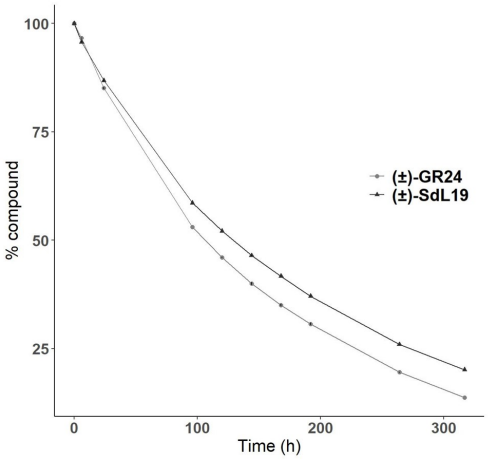


Figure 4. Stability of (±)-SdL19. Chemical hydrolysis of (±)-SdL19 and (±)-GR24 in ethanol/PBS at pH 6.8. Data are means ± SE (n = 3).

SLs and mimics are sensitive to hydrolysis giving for (±)-GR24 poorly active or inactive 5-hydroxy-3-methylbutenolide (D-OH)[51] and inactive ABC=CHOH tricycle[59]. Their sensitivity to hydrolysis has been tested routinely in aqueous solutions and compared to that of (±)-GR24[23,60], even though the assay was not performed at biologically active concentrations. Therefore, the chemical hydrolysis of (±)-SdL19 in comparison with (±)-GR24 was evaluated in a mixture of ethanol/water at pH 6.8, as previously reported for other SL analogs and mimics[23,60]. Under these conditions, a slightly higher stability of (±)-SdL19 was recorded in comparison with (±)-GR24 ((±)-SdL19 $t_{1/2} \approx 120$ h, (±)-GR24 $t_{1/2} \approx 100$ h) (Figure 4).

(±)-SdL19 cannalactone analog weakly interacts with the SL receptor PrKAI2d3. We have recently characterized the PrKAI2d3 protein as a SL receptor from *P. ramosa* 1 among five PrKAI2 candidates, and we have demonstrated its high interaction with (±)-GR24[51]. We tested the interaction between (±)-SdL19 and PrKAI2d3 using nano differential scanning fluorimetry (nanoDSF). NanoDSF allows to evaluate the interaction between a receptor protein and a ligand by monitoring the melting temperature of the receptor protein. In nanoDSF, changes in the protein fluorescence (ratio 350 nm/330 nm) are recorded and do not require a dye. This technique can highlight interactions that induce minor conformational changes. Compared to (±)-GR24, incubation with (±)-SdL19 at low concentrations did not affect the melting temperature of PrKAI2d3. However, the use of high concentrations of (±)-SdL19 lowered the inflection point of the melting curve indicating the binding of the ligand to the protein (Figure 5). We studied also the binding affinity of (±)-SdL19 towards PrKAI2d3 by intrinsic fluorescence but no K_d value was measurable in comparison with (±)-GR24 (Figure 6). The lower affinity of (±)-SdL19 for PrKAI2d3 in comparison with (±)-GR24 confirmed the nanoDSF data. These results are in accordance with the lower bioactivity of (±)-SdL19 on seeds of *P. ramosa* 1 in comparison with (±)-GR24. The characterization of SL receptor(s) from *P. ramosa* 2a is awaiting and would be appreciable to discuss the SAR results presented here in the light of ligand-protein interactions.

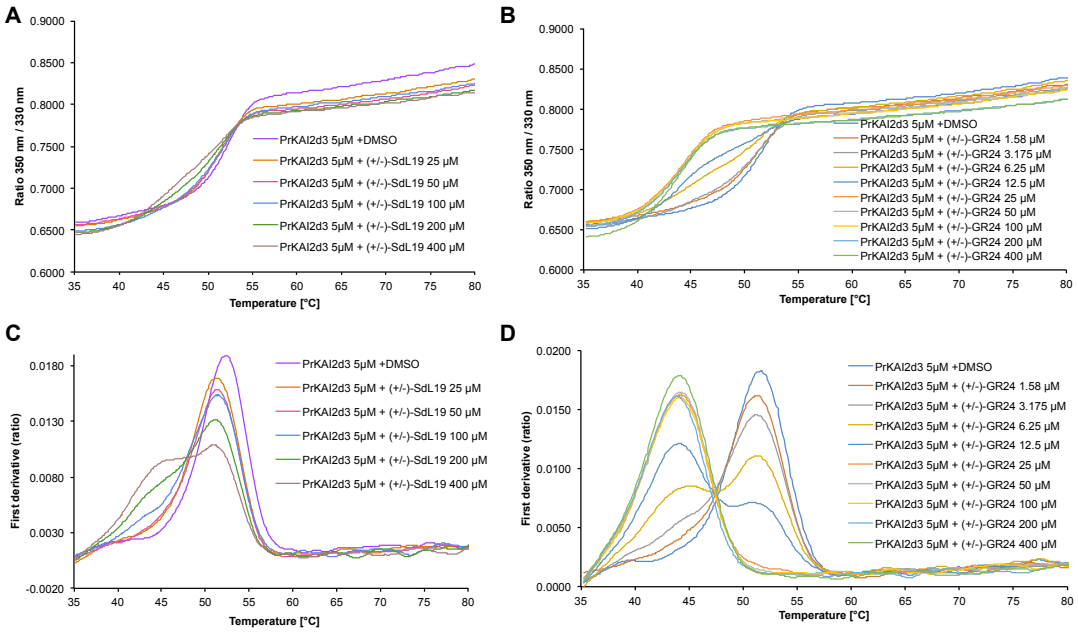


Figure 5. Biochemical analysis of the interaction between the PrKAI2d3 with (±)-GR24 and (±)-SdL19 by nanoDSF. **(A, B)** Thermostability of PrKAI2d3 at 5 µM in the absence of ligand or in the presence of various ligand concentrations. Panels **(A, B)** show the changes in fluorescence (ratio F_{350nm}/F_{330nm}) with temperature for (±)-SdL19 and (±)-GR24, respectively. The panels **(C, D)** show the first derivatives for the F_{350nm}/F_{330nm} curve against the temperature gradient from which the apparent melting temperatures (T_m) were determined for (±)-SdL19 and (±)-GR24, respectively. The experiment was carried out twice.

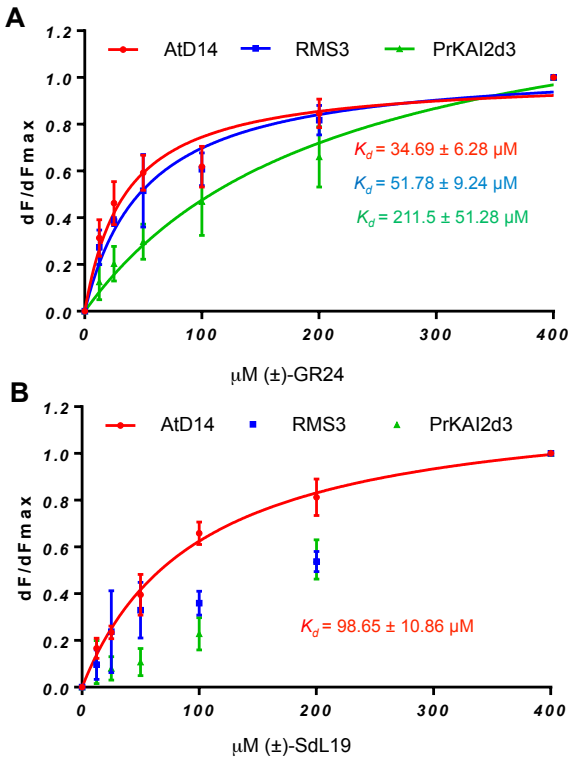


Figure 6. Biochemical analysis of the interaction between the PrKAI2d3, RMS3 and AtD14 proteins with (±)-GR24 (**A**) and (±)-SdL19 (**B**) by intrinsic tryptophan fluorescence. Plots of fluorescence intensity *versus* (±)-SdL19 or (±)-GR24 concentrations were used to determine the apparent K_d values. The plots represent the mean of two replicates and the experiments were repeated at least three times.

Cannalactone analogs efficiently inhibit bud outgrowth in pea and *Arabidopsis*, and interact with SL receptor D14 proteins. The biological activities of (±)-SdL analogs as plant hormones were evaluated using a pea branching assay with the highly branched SL-deficient *rms1-10* mutant[61]. All (±)-SdL analogs showed activity at a concentration of 1 µM but were found to be notably less active than (±)-GR24, since they were not significantly bioactive at 10 nM or below (Figure 7, Table S2). This confirms the low specificity of SL reception in pea for which a wide range of SLs, analogs and mimics are bioactive[23,60]. Moreover, (±)-SdL analogs were inactive on the branching of the pea *rms3-4* perception mutant (Figure 7**A)**, Table S3). These results suggest that (±)-SdL analogs, as (±)-GR24, are bioactive SL analogs and inhibit bud outgrowth via the RMS3 receptor, an ortholog of D14 in pea, and not because of toxicity. To investigate potential species differences, we examined the effect of (±)-SdL19 on *Arabidopsis* shoot branching. We applied (±)-SdL19 and (±)-GR24 to the hydroponically grown *max3-11* plants. *max3-11* is a SL-deficient mutant[62]. Treatment with all concentrations of (±)-SdL19 inhibited outgrowth of axillary buds in *max3-11*. However, a significant difference was observed with (±)-GR24 for low concentrations tested (< 3000 nM) (Figure 7**B**). These results indicated that (±)-SdL19 is less active than (±)-GR24 in *Arabidopsis* for shoot branching inhibition when applied to the roots in hydroponic culture.

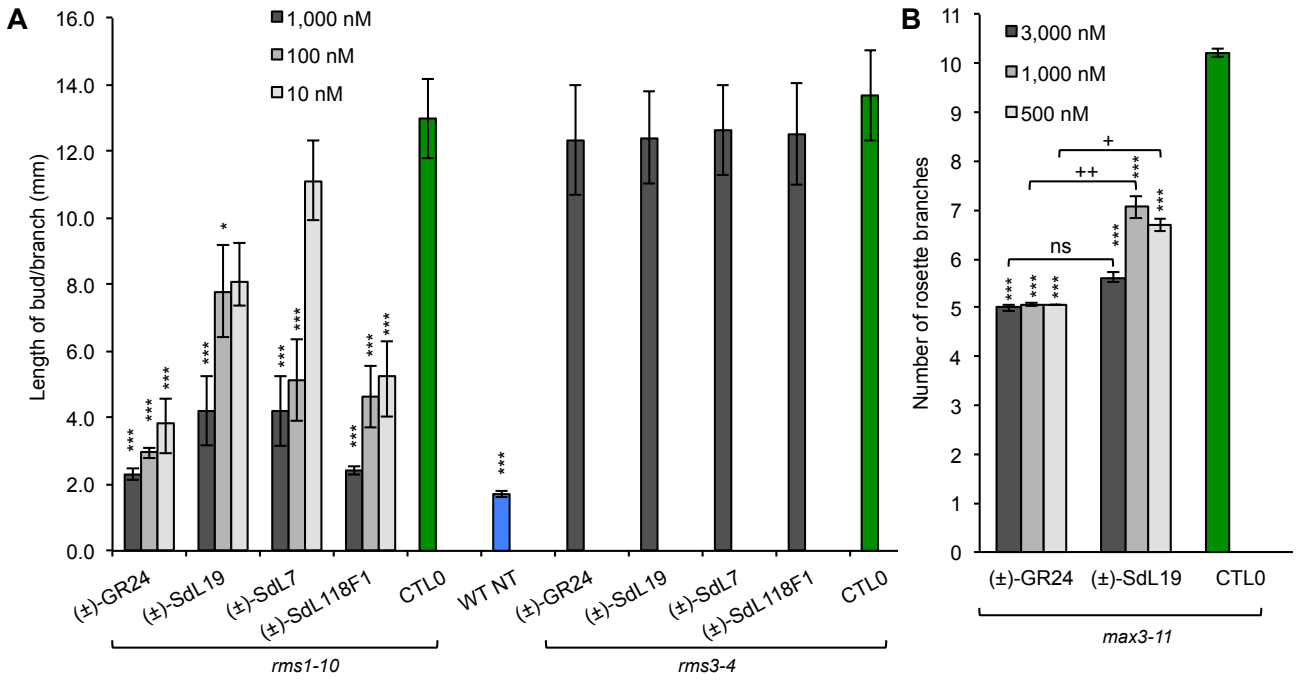


Figure 7. Bioactivity in pea and *Arabidopsis*. Bioactivity in pea of (±)-SdL7, (±)-SdL19 and (±)-SdL118F1 *versus* (±)-GR24 (*rms1, rms3*) (**A**). Length of the axillary buds of *rms1-10* and *rms3-5* pea plants, 8 d after direct application of the various analogs; CTL0 = DMSO treatment ; WT Térèse plants were used as controls without treatment. Data are means ± SE (≥ 20 plants) ***$P < 0.001$, *$P < 0.5$, Kruskal-Wallis rank sum test, compared to CTL0 value. See also supplementary data in the Supporting Information. Bioactivity in *Arabidopsis* of probes *versus* (±)-GR24 (*max3-11*). Bioactivity in *Arabidopsis* of (±)-SdL19 *versus* (±)-GR24 (**B**). Number of rosette branches of mutant plants *max3-11* grown in long-day conditions. These data were obtained from means ± SE ($n = 16$ plants). *** $P < 0.001$ indicate significant differences with the control treatment (0 nM) (CTL0) (Shapiro-Wilkinson normality test). + $P < 0.05$, ++ $P < 0.01$ indicate significant differences with (±)-GR24 treatment (Shapiro-Wilkinson normality test). ns = not significant. CTL0 = control 0.

In order to validate that (±)-SdL analogs are perceived by the pea SL receptor RMS3, we performed differential scanning fluorimetry (DSF) and revealed a shift in RMS3 melting temperature in the presence of (±)-SdL19, corresponding to a protein destabilization as for the other SL bioactive analogs[4] (Figure 8**A-B**). We showed that the destabilization of RMS3 by (±)-SdL19 was recorded at higher ligand concentrations in comparison with (±)-GR24 suggesting lower affinity. For AtD14, an ortholog of D14 in *Arabidopsis*, DSF recordings revealed an increased sensitivity for (±)-SdL19, inversely for (±)-GR24 as previously reported for cannalactone **14**[44] and in contrast to RMS3 (Figure 8**C-D)**. These results are in accordance with the fact that in pea, the main SLs detected are canonical SLs[63], while in *Arabidopsis*, no canonical SL has been detected but only non-canonical SLs or their biosynthetic precursors such as methyl carlactonoate ((+)-MeCLA **10**) and HO-MeCLAs[12,13]. Then, we estimated the binding affinity of (±)-SdL19 towards RMS3 and AtD14 by intrinsic fluorescence and found a measurable K_d value (98.65 ± 10.86 **µ**M) only for AtD14 (Figure 6**B**). The lower affinity of (±)-SdL19 for RMS3 in comparison with AtD14 highlights differences between biochemical and *in planta* results where in both *Arabidopsis* and pea, (±)-SdL19 is less bioactive than (±)-GR24 for bud outgrowth inhibition.

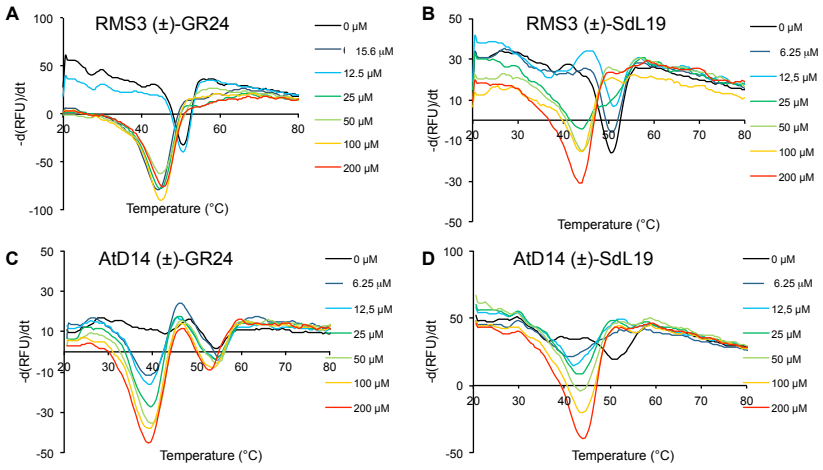


Figure 8. Biochemical analysis of the interaction RMS3/PsD14, AtD14 proteins with (±)-GR24 and (±)-SdL19. The melting temperature curves of RMS3 (**A, B**) and AtD14 (**C, D**) proteins with varying indicated concentrations of (±)-GR24 and (±)-SdL19, as assessed by DSF, are shown. Each line represents the average protein melt curve for three technical replicates and the experiment was carried out three times.

(±)-SdL19 cannalactone analog promotes hyphal branching in the AM fungus *Rhizophagus irregularis*. The SL analogs produced in the present study can also help to address SAR in AM symbiosis. SLs are known to induce a number of developmental, cellular and metabolic responses in AM fungi[34-36]. In particular, the stimulation of hyphal branching is commonly used in bioassays to detect the bioactivity of SLs on these fungi. Using this approach, a number of SLs and related compounds have been tested for their activity on the AM fungus *Gigaspora margarita*. Taken together, these studies highlighted the complexity of structural requirements in the ABC moiety. GR5 was shown to be inactive, and early studies proposed that a minimal structure would contain the C-D moiety fused to at least one ring system[35,64]. This proposal is consistent with the recent discovery of bioactive bryosymbiol **13** carrying A, C and D rings[22]. However, results obtained with CL derivatives later indicated that some compounds without a C ring could retain activity[26]. Combined with reports on natural non-canonical SLs bearing variations on the A or C rings[6], these studies indicate that requirements for bioactivity on AM fungi can be fulfilled in several divergent ways.

In the present study, we first used an *in vitro* assay which allows a quantification of hyphal branching[65] in the AM fungus *Rhizophagus irregularis*. As shown in Figure 9**A**, (±)-SdL19 stimulated hyphal branching (*i.e.* the formation of first-order and higher-order branches) in a similar fashion to (±)-GR24. This indicates that a C-D moiety combined with an acyclic carbon chain is sufficient for bioactivity on this AM fungus.

The hyphal branching response triggered by SL analogs is commonly used as a proxy measure for the stimulation of the fungal symbiont, but this response does not always reflect the ability of these compounds to facilitate the initiation of symbiosis[65]. To further document the ability of (±)-SdL19 to stimulate *R. irregularis* in a true symbiotic context, we used an additional test. This assay involves *Medicago truncatula* plants mutated in the SL biosynthesis gene *CCD8*. These mutants are strongly affected in their ability to initiate symbiosis with *R. irregularis*, and this phenotype can be rescued by exogenous application of SL analogs[65]. Like other bioassays involving SL biosynthesis plant mutants and designed to investigate the hormonal activities of SL analogs, this test records the ability of these analogs to "replace" natural SLs in a physiological context. Using this assay, we have previously shown the bioactivity of cannalactone **14** in AM symbiosis[44], indicating that the B ring is dispensable. In the present study, we found that (±)-SdL19 exhibited an activity similar to (±)-GR24 (Figure 9**B**). This extends our previous observations by showing that symbiotic activity can be conserved when both A and B rings are absent and replaced by an unsaturated acyclic carbon chain.

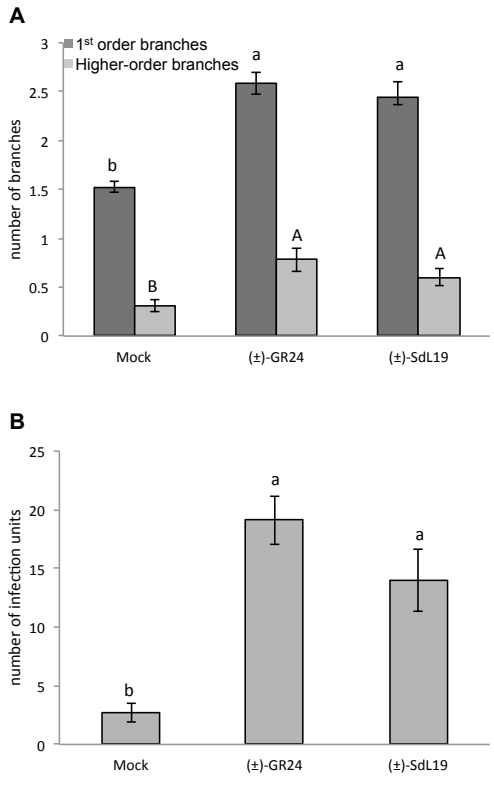


Figure 9. Activity of (±)-SdL19 on the development of *R. irregularis* and its symbiotic ability. (**A**) *R. irregularis* was grown from spores for 12 days on medium containing 10^{-7} M (±)-GR24 or (±)-SdL19, or the solvent alone (mock), then the number of branches of first order (black bars) and higher order (grey bars) were measured. Bars represent the mean ± SE, n = 6 to 8 plates per condition, representing an average of 200 spores. (**B**) *R. irregularis* spores were used to inoculate *M. truncatula ccd8-1* SL-deficient plants. 10^{-7} M (±)-GR24 or (±)-SdL19, or the solvent alone (mock) were supplied in the nutrient solution. The ability of (±)-SdL19 to restore symbiotic ability in *R. irregularis* was assessed by examining root colonization, 23 days post-inoculation. Bars represent the mean number of infection units per plant ± s.e.m. n = 14 to 16 plants per condition. Bars topped with the same letter do not differ significantly by Mann-Whitney U test ($P > 0.05$).

To conclude, we provide with this study comprehensive SAR data in two genetic groups of *P. ramosa*, comprising routes for synthesis of 14 analogs (SdL) of the non-canonical SL cannalactone **14**. The SdL analogues with the best specificity towards the population 2a are the compounds with a polar part on the side carbon chain. In addition to non-canonical SL cannalactone **14** recently identified from hemp in our group[44], natural canonical SLs (–)-solanacol **5** and (–)-solanacyl acetate **6** exuded by tobacco[41,42] and tomato[66], host plants for *P. ramosa* 2a[38,39], are reported here as remarkable selective germination stimulants for *P. ramosa* 2a seeds, contrary to other SLs such as orobanchol **2**, orobanchyl acetate **3** and 5-deoxystrigol **4,** also detected in tobacco root exudates[42]**.** Our data further extend common knowledge on SL analogs that are involved in plant and AM fungi development. Further studies on the interaction of those substances with specific receptors in AM fungi, key players for a sustainable agriculture, and in *P. ramosa* 2a, will help to fully resolve the structure**–**activity relationships in these species[65]. Moreover, these highly active non-canonical SLs (e.g., (±)-SdL19) could be useful for the study of other organisms which putatively produce only non-canonical SLs such as the moss *Physcomitrium patens*[6,67,68] and *Arabidopsis thaliana*[13].

EXPERIMENTAL SECTION

Synthesis: General experimental procedures*.* All non-aqueous reactions were run under an inert atmosphere (argon), by using standard techniques for manipulating air-sensitive compounds. All glassware was stored in the oven and/or was flame-dried prior to use. Anhydrous solvents were obtained by filtration through drying columns. Analytical thin-layer chromatographies (TLC) were performed on plates precoated with silica gel layers. Compounds were visualized by one or more of the following methods: (1) illumination with a short wavelength UV lamp (i.e., λ = 254 nm), (2) spray with a 1% (w/v) $KMnO_4$ solution in H_2O. All separations were carried out under flash-chromatographic conditions on silica gel (prepacked column, 230 – 400 mesh) at medium pressure (20 psi) with Armen fraction collector and pump. Nuclear magnetic resonance spectra (^1H; ^{13}C NMR) were recorded respectively at [500 or 300; 175, 125 or 75] MHz on recorded on Brucker Avance spectrometers at 298 K. For the ^1H spectra, data are reported as follows: chemical shift, multiplicity (s = singlet, d = doublet, t = triplet, q = quartet, m = multiplet, b = broad, coupling constant in Hz and integration. The numbering for signal assignment was done according to Chart 2. IR spectra are reported in reciprocal centimeters (cm^{-1}). Buffers and aqueous mobile-phases for UPLC were prepared using water purified with a Milli-Q system. Mass spectra (MS) and high-resolution mass spectra (HRMS) were determined by electrospray ionization (ESI) coupled to a time-of-flight analyzer (Waters LCT Premier XE, Waters, USA) or with an Ultra Performance Liquid Chromatography system equipped with a Triple Quadrupole mass spectrometer Detector (Acquity UPLC-TQD, Waters, USA).

All-*trans*-β-carotene **17** is commercially available. (±)-GR24 was prepared according to known procedures[69] and careful purification (HPLC)[45]. (±)-GR5 was synthesized by known procedures[21]. (±)-MeCLA was prepared by an unpublished method (Lucile Andna, Laurence Miesch). (±)-Carlactone was synthesized by Adrian Scaffidi[70]. Natural cannalactone **14** was isolated as described in Hamzaoui et al[44]. (±)-Strigol **1**, (±)-5-deoxystrigol **4**, (±)-sorgolactone **5**, (±)-orobanchol **2** are commercially available. Orobanchyl acetate **3** was synthesized from (±)-orobanchol by acetylation with acetic anhydride in pyridine as described in Boutet et al[71]. (–)-Solanacol **5** and (–)-solanacyl acetate **6** are obtained as described in Boyer et al[23] and (±)-7,8-desmethyl solanacol **15** and (±)-7,8-desmethyl solanacyl acetate **16** as described in Chen et al[72]. (±)-Fabacyl acetate **7** was kindly furnished by Koichi Yoneyama. (±)-4-Vinyldihydrofuran-2(*3H*)-one **19** was prepared by a known procedure[52].

(2'*R*,4R)-SdL4F1 and (2'*R*,4S**)-SdL4F2.** A mixture of alkene **19** (200 mg, 1.78 mmol), ethyl formate (144 µL, 1.96 mmol) in THF (4 mL) was placed at –78 °C. Potassium *tert*-butoxide was added (240 mg, 2.14 mmol). The mixture was stirred for 2 h at –78 °C. A solution of bromide derivative **20**[73] (350 mg, 1.96 mmol) in THF (3.2 mL) was added. The mixture was stirred at room temperature during 12 h. The mixture was diluted with EtOAc and saturated NH_4Cl aqueous solution and then separated. The organic phase was washed with water and brine. The combined organic layers were dried with Na_2SO_4, filtered and evaporated under reduced pressure. The mixture was purified by chromatography on silica gel (heptane/EtOAc 80: 20 to 60: 40 during 30 min) to afford pure (±)-SdL4F1 (87.5 mg, 21%) and (±)-SdL4F2 (85.7 mg, 20%) as a brown oils. (±)-SdL4F1: ^1H NMR (300 MHz, $CDCl_3$) δ: 7.51 (d, *J* = 2.0 Hz, H10), 6.88 (t, *J* = 1.5 Hz, H6'), 6.12 (t, *J* = 1.5 Hz, H2'), 5.81-5.70 (m, H6), 5.12 (dt, *J* = 1.0, 6.0 Hz, H7a), 5.08 (d, *J* = 1.0 Hz, H7b), 4.41 (t, *J* = 9.0 Hz, H5a), 4.07 (q, *J* = 4.5 Hz, H5b), 3.83-3.74 (m, H4), 1.97 (t, *J* = 1.5 Hz, 3 H7'). ^{13}C NMR (75 MHz, $CDCl_3$) δ: 171.5 (C5'), 170.4 (C2), 151.7 (C6'), 141.1 (C3'), 135.9 (C4'), 135.4 (C6), 116.7 (C7), 109.9 (C3), 100.7 (C2'), 71.1 (C5), 40.6 (C4), 10.9 (C7'). IR (cm^{-1}): 3092, 2983, 2919, 2850, 1781, 1752, 1683, 1344, 1207, 1184, 1083, 1026, 955, 866, 801 745. HRMS (ESI): Calcd for $C_{12}H_{13}O_5$ $[M + H]^+$: 237.0763, found: 237.0762. (±)-SdL4F2: ^1H NMR (300 MHz, $CDCl_3$) δ: 7.48 (d, *J* = 2.0 Hz, H10), 6.88 (t, *J* = 1.5 Hz, H6'), 6.12 (t, *J* = 1.5 Hz, H2'), 5.79-5.68 (m, H6), 5.10 (dt, *J*

= 1.0, 6.0 Hz, H7a), 5.06 (d, *J* = 1.0 Hz, H7b), 4.40 (t, *J* = 9.0 Hz, H5a), 4.05 (q, *J* = 4.5 Hz, H5b), 3.82-3.74 (m, H4), 1.96 (t, *J* = 1.5 Hz, 3 H7'). ^{13}C NMR (75 MHz, CDCl3) δ: 171.5 (C5'), 170.4 (C2), 151.4 (C6'), 141.3 (C3'), 136.0 (C4'), 135.1 (C6), 116.9 (C7), 110.0 (C3), 100.6 (C2'), 71.0 (C5), 40.5 (C4), 10.9 (C7'). IR (cm^{-1}): 3089, 2917, 2850, 1775, 1747, 1679, 1342, 1181, 1082, 1003, 950. HRMS (ESI): Calcd for $C_{12}H_{13}O_5$ [M + H]$^+$: 237.0768, found: 237.0762.

(2'*R,4*R**)-SdL7.** To a solution of (±)-SdL4F1 (76.5 mg, 0.32 mmol, 1 equiv) in CH_2Cl_2 (0.36 mL), was added methyl acrylate (0.294 mL, 3.24 mmol, 10 equiv) and Hoveyda-Grubbs II metathesis initiator (HGII) (10.9 mg, 0.016 mmol, 5 mol%) under argon. The mixture was stirred for 24 h at 50 °C in a closed flask with rodavis cap. The mixture was purified by chromatography on silica gel (heptane/EtOAc 40: 60) to afford pure (±)-SdL7 (54.4 mg, 57%, brown oil). ^{1}H NMR (300 MHz, $CDCl_3$) δ: 7.58 (d, *J* = 2.0 Hz, H6'), 6.87 (t, *J* = 2.0 Hz, H3'), 6.80 (dd, *J* = 8.0, 15.5 Hz, H6), 6.12 (t, *J* = 2.0 Hz, H2'), 5.88 (dd, *J* = 1.0, 15.5 Hz, H7), 4.46 (t, *J* = 8.5 Hz, H5a), 4.13 (dd, *J* = 3.5, 9.5 Hz, H5b), 4.00-3.90 (m, H4), 3.73 (s, 3 H9), 1.99 (s, 3 H7'). ^{13}C NMR (75 MHz, $CDCl_3$) δ: 170.6 (C2), 170.3 (C5'), 166.5 (C8), 152.7 (C6'), 144.3 (C6), 140.9 (C3'), 136.1 (C4'), 122.9 (C7), 108.5 (C3), 100.8 (C2'), 69.9 (C5), 52.0 (C9), 39.1 (C4), 10.9 (C7'). $J_{C2\text{-}H6'}$ = 2.0 Hz. IR (cm^{-1}): 3096, 2959, 2919, 2850, 1782, 1756, 1721, 1683, 1437, 1348, 1280, 1186, 1091, 1033, 1010, 956, 867, 748. HRMS (ESI): Calcd for $C_{16}H_{17}NO_7Na$ [M + CH_3CN + Na]$^+$: 358.0903, found: 358.0903.

4-(3-Oxobut-1-en-1-yl)dihydrofuran-2(*3H*)-one (21). To a solution of 4-vinyldihydrofuran-2(3H)-one **19** (400.4 mg, 3.57 mmol, 1 equiv) in CH_2Cl_2 (4 mL), was added buten-3-one (2.98 mL, 35.70 mmol, 10 equiv) and HGII (110.4 mg, 0.17 mmol, 5 mol%) under argon. The mixture was stirred for 24 h at 50 °C in a closed flask with rodavis cap. The mixture was purified by chromatography on silica gel (heptane/EtOAc 70 : 30 to 50 : 50 during 30 min) to afford pure ketone **21** as a brown oil (375.9 mg, 68%). ^{1}H NMR (300 MHz, $CDCl_3$) δ: 6.66 (dd, *J* = 7.5, 15.5 Hz, H6), 6.17 (dd, *J* = 1.0, 16.0 Hz, H7), 4.48 (dd, *J* = 7.5, 11.5 Hz, H5a), 4.08 (dd, *J* = 7.5, 11.5 Hz, H5b), 3.38 (sext, *J* =8.0 Hz, H4), 2.74 (dd, *J* = 7.5, 16.0 Hz, H3a), 2.44 (dd, *J* = 7.5, 16.0 Hz, H3b), 2.25 (s, 3 H9). ^{13}C NMR (75 MHz, $CDCl_3$) δ: 197.5 (C2), 175.4 (C8), 142.9 (C6) 132.5 (C7), 71.4 (C5), 38.6 (C4), 34.0 (C3), 27.8 (C9). IR (cm^{-1}): 3000, 2913, 1771, 1672, 1629, 1360, 1257, 1162, 1015, 979, 890, 838. UPLC-TQD (MS): *m/z* 155.2 ([M + H] $^+$, 100%).

(*E*)-4-(3-Hydroxy-3-methylbut-1-en-1-yl)dihydrofuran-2(*3H*)-one (21a). THF (20 mL) was added to anhydrous $CeCl_3$ (800.0 mg, 3.24 mmol, 1.4 equiv), dried by heating at 140 °C/30 rpm for 2 h, 0 °C. The mixture was stirred overnight under argon at room temperature. At this temperature, a solution of ketone **21** (357.3 mg, 2.32 mmol) in THF (11.5 mL) was added and stirred for 1 h. Then it was cooled to –70 °C and a solution of methylmagnesium chloride in THF (1.1 mL (3 M), 3.24 mmol, 1.4 equiv) was added by syringe. The reaction mixture was stirred until TLC indicated disappearance of starting material. The reaction was quenched with an aqueous 10% acetic acid solution (20 mL) and extracted with EtOAc (3 × 10 mL). The organic layer was washed with water (2 × 10 mL) and brine (10 mL). The combined organic layers were dried with Na_2SO_4, filtered and evaporated under reduced pressure to afford crude product **22a** as a brown oil (381.8 mg, 96%) used in the next step without further purification but which can be also purified by chromatography on silica gel (heptane/EtOAc 40: 60) to afford pure alcohol **22a**. ^{1}H NMR (300 MHz, CDCl3) δ: 5.75 (dd, *J* = 1.0, 15.5 Hz, H6), 5.59 (dd, *J* = 8.0, 15.5 Hz, H7), 4.41 (dd, *J* = 8.0, 10.0 Hz, H5a), 3.97 (t, *J* = 8.5 Hz, H5b), 3.19 (sext, J = 8.5, H4), 2.65 (dd, *J* = 8.5, 17.5 Hz, H3a), 2.34 (dd, *J* = 9.5, 17.5 Hz, H3b), 1.30 (s, 3 H9 and 3 H10). ^{13}C NMR (75 MHz, $CDCl_3$) δ: 176.7 (C2), 141.3 (C7), 124.5 (C6), 72.8 (C8), 70.7 (C5), 38.8 (C4), 34.8 (C3), 30.0 (C9 or C10), 20.4 (C9 or C10). IR (cm^{-1}): 3446, 2973, 2921, 1774, 1677, 1464, 1420, 1374, 1170, 1043, 1015, 975, 908, 839, 796, 690. UPLC-TQD (MS): *m/z* 93.1 (100%), 153.2 ([M – H_2O]$^+$, 90%).

Preparation of cyclopropylmagnesium bromide[74]. To a stirred suspension of magnesium turnings (300 mg, 12.30 mmol) in dry THF (2.0 mL) under argon was added commercially available cyclopropyl bromide (0.800 mL, 9.99 mmol) in dry THF (12.2 mL) dropwise at room temperature over 30 min. During this operation, the reaction continued refluxing without heating. After the addition of the halide was completed, the mixture was stirred at room temperature for 5 h. The titration was performed as described in Sugano et al[74].

(*E*)-4-(3-cyclopropyl-3-hydroxybut-1-en-1-yl)dihydrofuran-2(3*H*)-one (22b). Ground $CeCl_3$ (455.5 mg, 1.80 mmol, 1.4 equiv) was dried by heating at 140 °C/30 rpm for 2 h. Dry THF (11 mL) was added at 0°C. The mixture was stirred overnight under argon at room temperature. At this temperature, a solution of ketone **21** (204.8 mg, 1.32 mmol) in 4 mL of dry THF was added and left to stir for 1 h. Then it was cooled to –70 °C and cyclopropylmagnesium bromide (5.6 mL, 0.32 M, 1.80 mmol, 1.4 equiv) was added by syringe. The reaction mixture was left to stir until TLC indicated that no starting material remained. The reaction was quenched with an aqueous 10% acetic acid solution (10 mL) and extracted with EtOAc (3 × 10 mL). The organic layer was washed with water (2 × 10 mL) and brine (10 mL). The combined organic layers were dried (Na_2SO_4). Solvent was removed to afford crude product **22b** (266.4 mg, quantitative) used in the next step without further purification but which can be also purified by chromatography on silica gel (heptane/EtOAc 40: 60) to afford pure alcohol **22b**. ^{1}H NMR (300 MHz, $CDCl_3$) δ: 5.64 (s, H7), 5.62 (s, H6), 4.40 (t, *J* =8.5 Hz, H5a), 3.97 (t, *J* = 8.0 Hz, H5b), 3.19 (sext, *J* = 8.0 Hz, H4), 2.64 (dd, *J* = 8.5, 17.5 Hz, H3a), 2.33 (dd, *J* = 9.0, 17.5 Hz, H3b), 1.23 (s, 3H10), 1.01-0.92 (m, H9), 0.40 (d, *J* = 8.0 Hz, 2H11 or 2H12), 0.28 (d, *J* = 5.5 Hz, 2H11 or 2H12). ^{13}C NMR (75 MHz, $CDCl_3$) δ: 176.6 (C2), 139.0 (C7), 125.8 (C6), 72.8 (C5), 71.6 (C8), 38.9 (C4), 34.9 (C3), 27.5 (C10), 21.6 (C9), 1.1 (C11 or C12), 0.97 (C11 or C12). IR (cm^{-1}): 3446, 2921, 2851, 1777, 1462, 1423, 1373, 1171, 1045, 1016, 977, 737. HRMS (ESI): Calcd for $C_{11}H_{17}O_3$ [M + H]$^+$: 197.1178, found: 197.1180.

(*E*)-4-(3-Methyl-3-((trimethylsilyl)oxy)but-1-en-1-yl)dihydrofuran-2(*3H*)-one (23a). A mixture of alcohol **22a** (137 mg, 0.80 mmol) and TMS-imidazole (7.4 mL,

50.39 mmol, 62.6 equiv) were stirred at 50 °C under argon for 1 h. The mixture was stirred at room temperature for 1 h and diluted with heptane (20 mL). The organic layer was washed with brine (2 × 10 mL), dried with Na_2SO_4, filtered and evaporated under reduced pressure to afford pure product **23a** (136.2 mg, 70%). ^{1}H NMR (300 MHz, $CDCl_3$) δ: 5.66 (dd, *J* = 1.0, 15.5 Hz, H6), 5.46 (dd, *J* = 8.0, 15.5 Hz, H7), 4.38 (dd, *J* = 8.0, 9.0 Hz, H5a), 3.95 (t, *J* = 9.0 Hz, H5b), 3.16 (sext, *J* = 8.5, H4), 2.62 (dd, *J* = 8.0, 17.5 Hz, H3a), 2.31 (dd, *J* = 9.5, 17.5 Hz, H3b), 1.26 (s, 3 H9 and 3 H10), 0.07 (s, 9 H TMS). ^{13}C NMR (75 MHz, $CDCl_3$) δ: 176.7 (C2), 142.2 (C7), 123.8 (C6), 73.2 (C8), 72.8 (C5), 38.9 (C4), 34.7 (C3), 30.5 (C9 and C10), 2.7 (C TMS). IR (cm^{-1}): 2966, 2918, 1783, 1377, 1362, 1250, 1165, 1038, 1019, 972, 839, 755. UPLC-TQD (MS): *m/z* 153.3 ([M – OTMS]$^+$, 100%), 93.2 (90%).

(*E*)-4-(3-cyclopropyl-3-((trimethylsilyl)oxy)but-1-en-1-yl)dihydrofuran-2(3*H*)-one (23b). A mixture of alcohol **22b** (240.7 mg, 1.23 mmol) and TMS-imidazole (7.22 mL, 49.20 mmol, 40 equiv) were stirred at 50 °C under argon during 1 h. The mixture was stirred at room temperature during 1 h and diluted with 20 mL of heptane. The organic layer was washed with brine (2 × 10 mL), dried over Na_2SO_4 and evaporated. The mixture was purified by chromatography on silica gel (4 g, heptane/EtOAc 80:20) to afford pure product **23b** (222.4 mg, 67%). ^{1}H NMR (300 MHz, $CDCl_3$) δ: 5.62 (d, *J* = 15.5 Hz, H6), 5.52 (dd, *J* = 7.5, 15.5, H7), 4.40 (dd, *J* = 8.0, 9.0, H5a), 3.97 (t, *J* = 8.5, H5b), 3.18 (sext, *J* = 8.0, H4), 2.64 (dd, *J* = 8.5, 17.5 Hz, H3a), 2.33 (dd, *J* = 9.5, 17.5 Hz, H3b), 1.25 (s, 3 H10), 0.88-0.78 (m, H9), 0.35-0.25 (m, 2 H11 and 2 H12), 0.06 (s, 9 HTMS). ^{13}C NMR (75 MHz, $CDCl_3$) δ: 176.7 (C2), 140.4 (C7), 125.0 (C6), 74.0 (C8), 72.8 (C5), 38.9 (C4), 34.8 (C3), 27.3 (C10), 22.2 (C9), 2.7 (C11 or C12), 1.3 (C11 or C12). IR (cm^{-1}): 3007, 2958, 2894, 1785, 1702, 1420, 1372, 1250, 1209, 1165, 1095, 1065, 1018, 975, 887, 839, 754, 685. HRMS (ESI): Calcd for $C_{14}H_{24}O_3Si$ [M – OTMS]$^+$: 179.1072, found: 179.1070.

(2'*R,4*R**)-SdL18F1 and (2'*R**,4*S**)-SdL18F2.** A mixture of compound **23a** (363.4 mg, 1.5 mmol), ethyl formate (0.12 mL, 1.50 mmol, 1.0 equiv) in THF (3 mL) was placed at –78 °C. Potassium *tert*-butoxide was added (190.7 mg, 1.70 mmol, 1.13 equiv). The mixture was stirred for 2 h. A solution of bromide derivative **20** (286.7 mg, 1.60 mmol, 1.1 equiv) in THF (3 mL) was added. The mixture was stirred at room temperature for 12 h. The mixture was diluted with EtOAc and saturated NH_4Cl aqueous solution. The organic phase was washed with water and brine. The combined organic layers were dried with Na_2SO_4, filtered and evaporated under reduced pressure. The mixture was purified by chromatography on silica gel (heptane/EtOAc 80: 20 to 70: 30 in 20 min) to afford products (±)-SdL18F1 and (±)-SdL18F1 as brown oils ((±)-SdL18F1: 100.7 mg (18%) and (±)-SdL18F2: 86.0 mg (16%), total: 34%). (±)-SdL18F1: ^{1}H NMR (300 MHz, $CDCl_3$) δ: 7.50 (d, *J* = 2.5 Hz, H6'), 6.82 (t, *J* = 1.5 Hz, H3'), 6.08 (t, *J* = 1.5 Hz, H2'), 5.64 (d, *J* = 15.5 Hz, H7), 5.48 (dd, *J* = 7.5, 15.5 Hz, H6), 4.43 (t, *J* = 9.0 Hz, H5a), 4.06 (q, *J* = 4.0 Hz, H5b), 3.82-3.74 (m, H4), 1.99 (t, *J* = 1.5 Hz, 3 H7'), 1.27 (s, 3 H9 and 3 H10), 0.09 (s, 9 HTMS). ^{13}C NMR (75 MHz, $CDCl_3$) δ: 171.6 (C2), 170.3 (C5'), 151.6 (C6'), 141.4 (C3'), 141.0 (C7), 136.0 (C4'), 123.6 (C6), 110.6 (C3), 100.7 (C2'), 73.4 (C8), 71.5 (C5), 39.5 (C4), 30.7 (C9 or C10), 30.6 (C9 or C10), 10.9 (C7'), 2.8 (3C TMS). IR (cm^{-1}): 2967, 2925, 1785, 1754, 1683, 1380, 1344, 1250, 1183, 1082, 1031, 956, 840, 752. HRMS (ESI): Calcd for $C_{15}H_{17}O_5Na$ [M + Na - OTMS]$^+$: 317.1001, found: 317.1004. (±)-SdL18F2: ^{1}H NMR (300 MHz, $CDCl_3$) δ: 7.50 (d, *J* = 2.5 Hz, H6'), 6.88 (t, *J* = 1.5 Hz, H3'), 6.11 (t, *J* = 1.5 Hz, H2'), 5.63 (d, *J* = 15.5 Hz, H7), 5.45 (dd, *J* = 7.5, 15.5 Hz, H6), 4.42 (t, *J* = 9.0 Hz, H5a), 4.03 (q, *J* = 4.5 Hz, H5b), 3.81-3.72 (m, H4), 1.96 (t, *J* = 1.5 Hz, 3 H7'), 1.22 (s, 3 H9 or 3 H10), 1.20 (s, 3 H9 or 3 H10), 0.05 (s, 9 HTMS). ^{13}C NMR (75 MHz, $CDCl_3$) δ: 171.7 (C2), 170.3 (C5'), 151.6 (C6'), 141.5 (C3'), 141.1 (C7), 136.0 (C4'), 123.3 (C6), 110.5 (C3), 100.6 (C2'), 73.4 (C8), 71.5 (C5), 39.5 (C4), 30.7 (C9 or C10), 30.4 (C9 or C10) 10.8 (C7'), 2.7 (3C TMS). IR (cm^{-1}): 2967, 2925, 1786, 1755, 1683, 1380, 1344, 1264, 1183, 1084, 1032, 956, 840, 735. HRMS (ESI): Calcd for $C_{15}H_{17}O_5Na$ [M + Na - OTMS]$^+$: 317.1001, found: 317.0998.

(2'*R,4*R**)-SdL19.** To a solution of scandium trifluoromethanesulfonate (0.66 mg, 1.3 μmol) in CH_3CN (1.5 mL) was added silyl derivative (±)-SdL18F1 (98 mg, 0.27 mmol) in CH_3CN (1.0 ml) and water (2.5 μL, 0.14 μmol) at room temperature. The resulting mixture was stirred for 1 h at room temperature and quenched with a phosphate buffer (pH 7). The organic materials were extracted with dichloromethane (3 × 10 mL), the combined extracts were washed with brine, dried with Na_2SO_4, filtered and evaporated under reduced pressure to afford pure (±)-SdL19 (87.7 mg, quantitative). ^{1}H NMR (300 MHz, $CDCl_3$) δ: 7.50 (d, *J* = 2.5 Hz, H6'), 6.85 (t, *J* = 1.5 Hz, H3'), 6.10 (t, *J* = 1.5 Hz, H2'), 5.71 (d, *J* = 15.5 Hz, H7), 5.58 (dd, *J* = 7.5, 15.5 Hz, H6), 4.43 (t, *J* = 9.0 Hz, H5a), 4.07 (dd, *J* = 4.5, 9.0 Hz, H5b), 3.83-3.76 (m, H4), 1.99 (t, *J* = 1.5 Hz, 3 H7'), 1.29 (s, 3 H9 and 3 H10). ^{13}C NMR (75 MHz, $CDCl_3$) δ: 171.4 (C2), 170.2 (C5'), 151.6 (C6'), 140.9 (C3'), 140.3 (C7), 135.8 (C4'), 123.7 (C6), 110.2 (C3), 100.6 (C2'), 71.2 (C5), 70.5 (C8), 39.3 (C4), 29.8 (C9 and C10), 10.7 (C7'). IR (cm^{-1}): 3460, 2973, 2924, 2850, 1783, 1750, 1682, 1372, 1345, 1265, 1185, 1089, 1032, 1010, 956, 863, 735, 703. HRMS (ESI): Calcd for $C_{15}H_{18}O_6Na$ [M + Na]$^+$: 317.1001, found: 317.0994.

(2'*R,4*R**)-SdL21.** To a solution of scandium trifluoromethanesulfonate (0.56 mg, 1.14 μmol) in CH_3CN (1.3 mL) was added silyl derivative (±)-SdL18F2 (83.5 mg, 0.33 mmol) in CH_3CN (0.29 mL) and water (2.0 μL, 0.11 μmol) at room temperature. The resultant mixture was stirred for 1 h at room temperature and quenched with a phosphate buffer (pH 7). The organic materials were extracted with dichloromethane (3 × 5 mL), the combined extracts were washed with brine, dried with Na_2SO_4, filtered and evaporated under reduced pressure to afford pure (±)-SdL21 (59.7 mg, 89%). ^{1}H NMR (300 MHz, $CDCl_3$) δ: 7.50 (d, *J* = 2.5 Hz, H6'), 6.89 (t, *J* = 1.5 Hz, H3'), 6.11 (t, *J* = 1.5 Hz, H2'), 5.68 (d, *J* = 15.5 Hz, H7), 5.54 (dd, *J* = 7.5, 15.5 Hz, H6), 4.43 (t, *J* = 9.0 Hz, H5a), 4.04 (dd, *J* = 4.5, 9.0 Hz, H5b), 3.82-3.74 (m, H4), 1.97 (t, *J* = 1.5 Hz, 3 H7'), 1.22 (s, 3 H9 and 3 H10). ^{13}C NMR (75 MHz, $CDCl_3$) δ: 171.6 (C2), 170.4 (C5'), 151.7 (C6'), 141.1 (C3'), 140.7 (C7), 135.9 (C4'), 123.7 (C6), 110.6 (C3), 100.7 (C2'), 71.4 (C5), 70.7 (C8), 39.4 (C4), 29.9 (C9 and C10), 10.8 (C7'). IR

(cm^{-1}): 3488, 2969, 2925, 1784, 1751, 1682, 1343, 1263, 1185, 1084, 1026, 1013, 955, 863, 802, 730, 701. HRMS (ESI): Calcd for $C_{15}H_{18}O_6Na$ [M + Na]$^+$: 317.1001, found: 317.1000. IR (cm^{-1}): 3488, 2969, 2925, 1784, 1751, 1682, 1343, 1263, 1185, 1084, 1026, 1013, 955, 863, 802, 730, 701. HRMS (ESI): Calcd for $C_{15}H_{18}O_6Na$ [M + Na]$^+$: 317.1001, found: 317.1000.

(2'*R,4*R**)-SdL33.** To a solution of (±)-SdL19 (15.6 mg, 0.05 mmol) in 0.3 mL of CH_2Cl_2 was added pyridine (0.09 mL, 1.06 mmol, 20 equiv), 4-nitrobenzoylchloride (49.2 mg, 0.26 mmol, 5 equiv) and DMAP (tip of spatula). The mixture was stirred overnight at 40 °C. The mixture was co-evaporated with toluene, extracted with EtOAc, washed with $NaHCO_3$ and dried with Na_2SO_4, filtered and evaporated under reduced pressure. The product was purified by PTLC (heptane/EtOAc 60: 40) to afford pure (±)-SdL33 (18.2 mg, 77%, yellow amorphous solid). ^{1}H NMR (300 MHz, $CDCl_3$) δ: 8.26 (dt, *J* = 2.0, 8.5 Hz, H14 and H14'), 8.11 (dt, *J* = 2.0, 8.5 Hz, H13 and H13'), 7.51 (d, *J* = 2.5 Hz, H6'), 6.89 (t, *J* = 1.5 Hz, H3'), 6.10 (t, *J* = 1.5 Hz, H2'), 5.98 (dd, *J* = 1.0, 15.5 Hz, H7), 5.63 (q, *J* = 8.0 Hz, H6), 4.45 (t, *J* = 8.5 Hz, H5a), 4.10 (t, *J* = 7.5 Hz, H5b), 3.87-3.79 (m, H4), 2.02 (s, 3 H7'), 1.23 (t, *J* = 7.0 Hz, 3 H9 and 3 H10). ^{13}C NMR (175 MHz, $CDCl_3$) δ: 171.4 (C2), 170.3 (C5'), 163.5 (C11), 151.8 (C6'), 150.6 (C15), 141.1 (C3'), 136.4 (C7), 131.5 (C4'), 130.7 (C13 and C13'), 126.8 (C6), 123.8 (C12), 123.7 (C14 and C14'), 110.0 (C3), 100.6 (C2'), 82.2 (C8), 71.2 (C5), 39.6 (C4), 27.3 (C9 or C10), 27.1 (C9 or C10), 11.0 (C7'). IR (cm^{-1}): 2919, 2850, 1785, 1755, 1722, 1683, 1607, 1527, 1464, 1349, 1290, 1185, 1102, 1033, 1014, 956, 876, 842, 720. HRMS (ESI): Calcd for $C_{22}H_{21}NO_9Na$ [M + Na]$^+$: 466.1114, found: 466.1131.

(2'*R,4*S**)-SdL34.** To a solution of (±)-SdL21 (15.6 mg, 0.05 mmol) in 0.3 mL of CH_2Cl_2 was added pyridine (0.09 mL, 1.06 mmol, 20 equiv), 4-nitrobenzoylchloride (49.17 mg, 0.265 mmol, 5 equiv) and DMAP (tip of spatula). The mixture was stirred overnight at 40 °C. The mixture was co-evaporated with toluene, extracted with EtOAc, washed with $NaHCO_3$ and dried with Na_2SO_4, filtered and evaporated under reduced pressure. The product was purified by PTLC (heptane/EtOAc 60: 40) to afford pure (±)-SdL34 (6.8 mg, 25%, yellow amorphous solid). ^{1}H NMR (300 MHz, $CDCl_3$) δ: 8.25 (dt, *J* = 2.0, 8.5 Hz, H14 and H14'), 8.10 (dt, *J* = 2.0, 8.5 Hz, H13 and H13'), 7.50 (d, *J* = 2.5 Hz, H6'), 6.92 (t, *J* = 1.5 Hz, H3'), 6.11 (t, *J* = 1.5 Hz, H2'), 5.96 (dd, *J* = 1.0, 15.5 Hz, H7), 5.60 (q, *J* = 8.0 Hz, H6), 4.46 (t, *J* = 8.5 Hz, H5a), 4.09 (t, *J* = 7.5 Hz, H5b), 3.87-3.79 (m, H4), 2.02 (s, 3 H7'), 1.24 (t, *J* = 7.0 Hz, 3 H9 and 3 H10). ^{13}C NMR (175 MHz, $CDCl_3$) δ: 171.3 (C2), 170.3 (C5'), 163.5 (C11), 151.8 (C6'), 150.6 (C15), 141.2 (C3'), 136.6 (C7), 135.4 (C4'), 130.8 (C13 and C13'), 126.6 (C6), 125.2 (C12), 123.7 (C14 and C14'), 110.1 (C3), 100.7 (C2'), 82.2 (C8), 71.1 (C5), 39.7 (C4), 27.1 (C9 or C10), 27.0 (C9 or C10), 10.9 (C7'). IR (cm^{-1}): 2919, 2850, 1784, 1754, 1722, 1683, 1607, 1527, 1464, 1349, 1289, 1184, 1101, 1032, 1013, 955, 875, 842, 721. HRMS (ESI): Calcd for $C_{24}H_{24}N_2O_9Na$ [M + CH_3CN + Na]$^+$: 507.1380, found: 507.1389.

(2'*R,4*S**)-SdL50.** To a solution of (±)-SdL21 (34.3 mg, 0.117 mmol) in CH_2Cl_2 (0.6 mL) was added pyridine (0.189 mL, 2.34 mmol, 20 equiv), 3,5-dinitrobenzoyl chloride (134.9 mg, 0.58 mmol, 5 equiv) and DMAP (tip of spatula). The mixture was stirred at 40 °C overnight. The mixture was co-evaporated with toluene, extracted with EtOAc, washed with $NaHCO_3$ and dried with Na_2SO_4. The product was purified by PTLC (heptane/EtOAc 45: 55) to afford pure (±)-SdL50 as a white solid (17.7 mg, 31%). ^{1}H NMR (300 MHz, $CDCl_3$) δ: 9.19 (t, *J* = 2.0 Hz, H15), 9.04 (d, *J* = 2.0 Hz, H13 and H13'), 7.52 (d, *J* = 2.5 Hz, H6'), 6.94 (t, *J* = 1.5 Hz, H3'), 6.12 (t, *J* = 1.5 Hz, H2'), 5.96 (dd, *J* = 1.0, 16.0 Hz, H7), 5.65 (dd, *J* = 7.5, 15.5 Hz, H6), 4.46 (t, *J* = 9.0 Hz, H5a), 4.08 (t, *J* = 5.0 Hz, H5b), 3.89-3.81 (m, H4), 2.02 (s, 3 H7'), 1.65 (s, 3 H9 or 3 H10), 1.62 (s, 3 H9 or 3 H10). ^{13}C NMR (125 MHz, $CDCl_3$) δ: 206.3 (C11), 171.2 (C5'), 170.2 (C2), 152.0 (C6'), 148.8 (C12), 141.1 (C3'), 135.8 (C7), 132.3 (C14 and C14'), 129.5 (C13 and C13'), 127.4 (C6), 122.4 (C15), 109.9 (C4'), 100.9 (C2'), 71.1 (C8), 67.2 (C5), 39.5 (C4), 29.9 (C3), 27.2 (C9 or C10), 26.8 (C9 or C10), 10.9 (C7'). R (cm^{-1}): 2985, 1737, 1447, 1373, 1301, 1233, 1098, 1043, 938, 918, 847, 786. HRMS (ESI): Calcd for $C_{24}H_{23}N_3O_{11}Na$ [M + CH_3CN + Na]$^+$: 552.1230, found: 552.1226.

(2'*R,4*R**)-SdL51.** To a mixture of (±)-SdL19 (21.8 mg, 0.07 mmol) and pyridine (250 µL, 3.09 mmol, 41.7 equiv) was added acetic anhydride (250 µL, 2.64 mmol, 35.7 equiv) and DMAP (tip of spatula). The mixture was stirred at room temperature under argon overnight. The product was co-evaporated with toluene and purified by PTLC (heptane/EtOAc 45: 55) to afford pure (±)-SdL51 (10.2 mg, 41%). ^{1}H NMR (300 MHz, $CDCl_3$) δ: 7.51 (d, *J* = 2.5 Hz, H6'), 6.95 (t, *J* = 1.5 Hz, H3'), 6.09 (t, *J* = 1.4 Hz, H2'), 5.83 (dd, *J* = 1.0, 15.5 Hz, H7), 5.48 (dd, *J* = 8.0, 15.5 Hz, H6), 4.43 (t, *J* = 8.5 Hz, H5a), 4.03 (t, *J* = 5.0 Hz, 5Hb), 3.83-3.74 (m, H4), 1.95 (s, 3 H7'), 1.46 (d, *J* = 4.0 Hz, 3 H9 and 3 H10), 1.23 (t, *J* = 7.0 Hz, 3 H12). ^{13}C NMR (175 MHz, $CDCl_3$) δ: 171.4 (C11), 170.5 (C2), 170.0 (C5') 151.9 (C6'), 141.4 (C3'), 137.3 (C7), 135.8 (C4'), 125.8 (C6), 109.7 (C3), 100.7 (C2'), 80.0 (C8), 71.3 (C5), 39.6 (C4), 27.3 (C9 or C10), 27.1 (C9 or C10), 14.4 (C12), 10.9 (C7'). IR (cm^{-1}): 2985, 1737, 1447, 1373, 1301, 1234, 1097, 1043, 938, 918, 847, 786. HRMS (ESI): Calcd for $C_{17}H_{20}O_7Na$ [M + Na]$^+$: 359.1107, found: 359.1109.

(2'*R,4*R**)-SdL118F1 and (2'*R**,4*S**)-SdL118F2.** A mixture of compound **23b** (150.8 mg, 0.56 mmol), ethyl formate (0.09 mL, 1.12 mmol, 2 equiv) in THF (1.2 mL) was placed at –78°C. Potassium *tert*-butoxide was added (142.5 mg, 1.27 mmol, 2.26 equiv). The mixture was stirred during 2 h. A solution of bromide derivative **20** (106.2 mg, 0.60 mmol, 1.08 equiv) in THF (1.2 mL) was added. The mixture was stirred at room temperature for 12 h. The mixture was diluted with EtOAc and saturated NH_4Cl aqueous solution. The organic phase was washed with water and brine. The combined organic layers were dried with Na_2SO_4, filtered and evaporated under reduced pressure. The mixture was purified by chromatography on silica gel (heptane/EtOAc 80: 20 to 70: 30 in 20 min) to afford pure products (±)-SdL118F1 and (±)-SdL118F2 ((±)-SdL118F1: 52.3 mg (24%), (±)-SdL118F2: 66.3 mg (30%), total: 54%). (±)-SdL118F1: ^{1}H NMR (300 MHz, $CDCl_3$) δ: 7.51 (d, *J* = 2.5 Hz, H6'), 6.84 (quint, *J* = 1.5 Hz, H3'), 6.08 (dd, *J* = 1.0, 3.0 Hz, H2'), 5.52 (t, *J* =5.5 Hz, H7 and H6), 4.43 (td, *J* = 2.0, 15.5 Hz, H5a), 4.10 (q, *J* = 7.0 Hz,

H5b), 3.81-3.74 (m, H4), 1.99 (t, *J* = 1.5 Hz, 3 H7'), 1.27 (s, 3 H10), 0.91-0.82 (m, H9), 0.34-0.24 (m, 2 H11 and 2 H12), 0.07 (s, 9 HTMS). ^{13}C NMR (75 MHz, $CDCl_3$) δ: 173.2 (C2), 169.1 (C5'), 151.6 (C6'), 141.0 (C3'), 140.9 (C7), 138.9 (C4'), 125.1 (C6), 110.1 (C3), 100.8 (C2'), 73.9 (C8), 71.5 (C5), 39.7 (C4), 27.7 (C10), 22.6 (C9), 10.9 (C7'), 2.7 (3C TMS), 1.5 (C11 and C12). IR (cm^{-1}): 2959, 1784, 1755, 1684, 1346, 1249, 1185, 1093, 1019, 1028, 955, 863, 841, 754. HRMS (ESI): Calcd for $C_{20}H_{28}O_6SiNa$ $[M + Na]^+$: 415.1553, found: 415.1547. (±)-SdL118F2: ^{1}H NMR (300 MHz, $CDCl_3$) δ: 7.51 (t, *J* = 1.5 Hz, H6'), 6.87 (sext, *J* = 1.0 Hz, H3'), 6.09 (q, *J* = 1.5 Hz, H2'), 5.52-5.49 (m, H7 and H6), 4.43 (td, *J* = 2.0, 15.5 Hz, H5a), 4.03 (q, *J* = 7.0 Hz, H5b), 3.81-3.74 (m, H4), 1.97 (q, *J* = 1.5 Hz, 3 H7'), 1.23 (s, 3 H10), 0.88-0.77 (m, H9), 0.28-0.21 (m, 2 H11 and 2 H12), 0.05 (s, 9 HTMS). ^{13}C NMR (125 MHz, $CDCl_3$) δ: 171.3 (C2), 170.2 (C5'), 151.3 (C6'), 141.0 (C3'), 140.9 (C7), 134.8 (C4'), 126.7 (C6), 113.6 (C3), 100.5 (C2'), 74.3 (C8), 71.5 (C5), 40.2 (C4), 29.9 (C10), 21.2 (C9), 10.9 (C7'), 5.7 (3C TMS), 1.5 (C11 and C12). Carbonyl resonances are missing in ^{13}C NMR spectra of (±)-SdL118F1 and (±)-SdL118F2 and found by HMBC spectra. IR (cm^{-1}): 2969, 1784, 1760, 1685, 1346, 1248, 1185, 1086, 1030, 1007, 956, 839, 750. HRMS (ESI): Calcd for $C_{20}H_{28}O_6SiNa$ $[M + Na]^+$: 415.1553, found: 415.1540.

(2'*R,4*R**)-SdL127.** To a solution of silyl ether (±)-SdL118F1 (23.0 mg, 0.06 mmol, 1 equiv) in CH_3CN (0.1 mL), was added acetic anhydride (0.011 mL, 0.12 mmol, 2 equiv) and scandium trifluoromethanesulfonate (0.29 mg, 0.59 μmol) under argon. The mixture was stirred for 2 h at room temperature under argon. The mixture was purified by PTLC (heptane/EtOAc 40: 60) to afford pure alcohol (±)-SdL127 as a colorless oil (1.8 mg, 19%). ^{1}H NMR (300 MHz, $CDCl_3$) δ: 7.50 (t, *J* = 3.0 Hz, H6'), 6.87 (dt, *J* = 1.5, 9.5 Hz, H3'), 6.09 (s, H2'), 5.62 (dq, *J* = 3.5, 15.5 Hz, H7), 5.51 (dd, *J* = 7.0, 15.5 Hz, H6), 4.43 (td, *J* = 2.0, 9.0 Hz, H5a), 4.05 (dd, *J* = 4.0, 9.0 Hz, H5b), 3.83-3.75 (m, H4), 1.99 (s, 3 H7'), 1.28 (s, 3 H10), 0.89-82 (m, H9), 0.43-0.34 (m, 2 H11 or 2 H12), 0.28-0.22 (m, 2 H11 or 2 H12). ^{13}C NMR (125 MHz, $CDCl_3$) δ: 171.5 (C2), 170.3 (C5'), 151.7 (C6'), 141.0 (C3'), 137.6 (C6), 136.2 (C4'), 125.9 (C7), 110.5 (C3), 100.8 (C2'), 72.0 (C8), 71.4 (C5), 39.7 (C4), 28.1 (C10), 22.0 (C9), 10.9 (C7'), 1.5 (C11 or C12), 0.9 (C11 or C12). IR (cm^{-1}): 3468, 2958, 2925, 2856, 1780, 1745, 1680, 1459, 1369, 1344, 1263, 1183, 1083, 1029, 1007, 953, 864, 798, 741, 672. HRMS (ESI): Calcd for $C_{17}H_{20}O_6Na$ $[M + Na]^+$: 347.1158, found: 347.1157.

X-ray Diffraction. Thin colorless needle 0.30 × 0.04 × 0.03 mm was mounted on a nylon loop with protection Paratone® oil. Cell dimensions and intensities were measured at 203 K on a RIGAKU diffractometer constituted by a MM007 HF rotating-anode generator, delivering intense Cu(K$_\alpha$) radiation (λ = 1.54187Å) through Osmic CMF confocal optics, and a Rapid II curved Image Plate detector allowing data measurement up to 2θmax = 144°; Clearly, the tiny crystals obtained by dissolving in ethyl acetate (48e)/ heptane (58e) and slow cooling of the solution turned out to be poor diffractors and a compromise was chosen between reasonable exposure time and exploitable data for model solution. 10732 measured reflections up to the θ value matching the *iUCR* criteria, 4562 independent reflections (*R*int = 0.138) of which only 687 had $|F_o| > 4\sigma$ (F_o) using the *CrystalClear 2.0* suite[75]. Data were corrected for Lorentz and polarization effects and for absorption ($T_{min, max}$: 0.448, 1.000). Despite the little signal detected beyond the 1.4 Å resolution limit, the structure could be readily solved either by dual methods (SHELXD)[76], or intrinsic phasing methods (*SHELXT* program[77]; all other calculations regarding the model refinement were performed with *SHELXL* system[78] and *PLATON*[79] programs, keeping meaningful X-ray diffraction intensities. A potential solvent accessible region with disordered electron density was detected within the crystal structure. *SQUEEZE*[80] was used to model the unresolved electron density likely resulting from disordered crystallizing solvent molecules, representing a total of 44 electrons per unit cell. This contribution was not included in the crystal data. Full-matrix least-squares refinement based on *F* using the weight of $1/[\sigma^2(F_o) + 0.2(F_o^2)]$ gave final values of *R1* = 0.101, *ωR2* = 0.269, and GOF(*F*) = 1.241 for 319 parameters, 276 restraints on the thermal parameters for all the non-H atoms with the *SHELXL* RIGU command and 1012 contributing reflections. Maximum shift/error = 0.0000, max/min residual electron density = 0.283/-0.210 e.Å^{-3}. Hydrogen atoms were placed in calculated positions (C—H = 0.94-1.00 Å) and refined as riding on their parent atoms, with U_{iso}(H) values constrained to 1.2 U_{eq}(C) or 1.5 Ueq (C_{methyl}). See Tables S1.

Plant material and growth conditions. Pea (*Pisum sativum*) branching mutants used in this study were derived from various cultivars of pea after ethyl methanesulfonate (EMS) mutagenesis and were described previously[81]. The *rms1-10* (M3T-884) and *rms3-4* (M2T-30) mutants were obtained from the dwarf cv Térèse. Plants were grown in a greenhouse under long days as described in Braun et al.[82].

All *A. thaliana* plants used in this study originated from the Columbia (Col-0) ecotype background and have been described previously: *max3-11*[62]. Plants were grown as described in Cornet et al.[83] for a hydroponic assay (see also below).

Two batches of parasitic plant seeds were used in this study. A population of seeds of *Phelipanche ramosa* (L.) Pomel associated to genetic group 1 (*P. ramosa* 1) was collected from Saint Martin-de-Fraigneau, France, on broomrape parasitizing winter oilseed rape (*Brassica napus* L.) in 2015. Seeds of *P. ramosa* from genetic subclade 2a (*P. ramosa* 2a) were harvested at Saint Martin-de-Bossenay, France, on broomrape developed on hemp (*Cannabis sativa* L.) in 2012[38]. Seeds were surface sterilized and conditioned according to Pouvreau et al.[57] (dark condition; 21 °C).

Pea shoot branching assay. The compounds to be tested were applied directly to the axillary bud with a micropipette as 10 µL of a solution containing 0.1% DMSO with 2% polyethylene glycol 1450, 50% ethanol and 0.4% DMSO[23,84]. The control-0 is the treatment with 0.1% DMSO without compound. 24 plants were sown per treatment in trays (2 repetitions of 12 plants). The treatment was generally performed 10 days after sowing, on the axillary bud at node 3. The branches at nodes 1 to 2 were removed to encourage the outgrowth of axillary

buds at nodes above. Nodes were numbered acropetally from the first scale leaf as node 1 and cotyledonary node as node 0. Bud growth at node 3 was measured with digital callipers 8 to 10 days after treatment. Plants with a damaged main shoot apex or showing a dead white treated-bud were excluded from the analysis. The SL-deficient *rms1-10* and SL-reception *rms3-4* pea mutants were used for all experiments and WT Térèse was used as control.

Hydroponic assay on *Arabidopsis*. The hydroponic assay was adapted from Cornet et al.[83]. Seeds were surface-sterilized for 8 min in a solution of ethanol (95%)-Bayrochlore (Bayrol, Mundolsheim, France) (10%), and were rinsed twice with ethanol (100%). Each seed was sown on top of a cut 0.5 mL Eppendorf tube filled with agar medium containing 0.65% agar and 10% nutritive solution 5 mM NO_3. Tubes were soaked in water and stored in the dark at 4 °C for 2 d. Twelve plants per pipette tip box (13 × 9 × 7 cm) were grown and supplied with nutrient solution as in Boyer et al.[60] at a concentration of 5 mL.L^{-1} (750 mL of solution per box). Every week the nutrient solution was renewed and every ten days when the molecules were added into the solution. The first treatment occurred at day 27 after sowing when plants started to bolt. The number of rosette branches was performed at day 42.

Germination stimulation activity assay on root parasitic plant seeds. Germination Stimulant activity (GS) of chemicals on seeds of parasitic plants were determined using a method described previously[57,85]. Chemicals were suspended in DMSO, except all-*trans*-β-carotene **17** in THF, at 10 mmol.L^{-1}, then diluted with water at 1 mmol.L^{-1} (water/DMSO; v/v; 9/1). Dilutions of 1×10^{-5} mol.L^{-1} to 1×10^{-12} mol.L^{-1} were then performed in water/DMSO (v/v; 9/1). For each compound, a range of concentrations from 10^{-13} to 10^{-6} mol.L^{-1} (water/DMSO; 99/1) were applied to conditioned parasitic seeds. DMSO 1% was used as negative control (seed germination < 1%) and (±)-GR24 at a concentration of 1 µmol.L^{-1} was used as a positive control and induced 72-87% of seed germination for *P. ramosa* 1, 80–90% for *P. ramosa* 2a. To avoid variations related to sterilization events percentages of germination are reported as a ratio relative to the positive control ((±)-GR24, 1 µmol L^{-1}) included in each germination assay. Each dilution and germination assay was repeated at least three times. For each compound tested, dose-response curves (Germination stimulation = f(c), Germination Stimulant activity relative to (±)-GR24 1 µmol L^{-1} ; c : concentration (mol. L^{-1}), half maximal effective concentration (EC_{50}), and maximum of germination stimulant activity were determined using a Four Parameter Logistic Curve computed with SigmaPlot® 10.0.

Fungal material. *Rhizophagus irregularis* spores (strain DAOM197198) were purchased from Agronutrition (France). They were rinsed twice with sterile water before use.

Analysis of hyphal branching *in vitro*. Experiments were carried out as described in Taulera et al. (2020)[65]. Spores were placed on plates containing M medium[86] and supplemented with SL analogs (100 nM.L^{-1}), or 0.1% DMSO for mock treatments. Plates were incubated at 30 °C under 2% CO_2 for 12 days. Germ tubes were then identified as the longest hypha coming out of each spore. The number of hyphal branches of the 1st order (growing from the germ tube) and higher order (growing from 1st-order branches) was scored using a dissecting microscope for each germinated spore. The average number of branches of each order was calculated for all the germinated spores on a plate (typically 25 to 35 spores). For statistical analysis, each plate was treated as a replication unit (represented by the plate mean), and 6 to 8 plates were analyzed for each treatment.

Symbiosis initiation assay. The assay was carried out as described in Taulera et al.[65]. Briefly, *ccd8-1* mutants of *Medicago truncatula*[87] were grown on a clay substrate inoculated with 150 spores of *R. irregularis*. SL analogs were added to the nutrient solution, to reach a final concentration of 100 nM.L^{-1}. Mock treatments were performed with 0.1% DMSO. The number of infection points in each root system was recorded three weeks post-inoculation, after staining fungal structures with ink.

Expression and purification of proteins. Expression and purification of proteins RMS3, AtD14, and PrKAI2d3 with a cleavable GST tag were performed in accordance with de Saint Germain et al.[51,61].

Differential Scanning Fluorimetry (DSF). DSF experiments were performed on a CFX384 Touch™ Real-Time PCR Detection System (Biorad) using excitation and emission wavelengths of 490 and 575 nm, respectively. Sypro Orange ($\lambda_{Ex}/\lambda_{Em}$: 490/610 nm; Life technologies) was used as the reporter dye. Samples were heat-denatured using a linear 25 to 95 °C gradient at a rate of 1.3 °C per minute after incubation at 25 °C for 30 min in the absence of light. The denaturation curve was obtained using CFX manager software. Final reaction mixtures were prepared in triplicate in 384-well white microplates, and each reaction was carried out in 20-µL scale in PB buffer pH 6.8 containing 10 µg protein, each concentration of SL derivatives (DMSO solution, final DMSO concentration was 4%), and 0.008 µL Sypro Orange. In the control reaction, DMSO was added instead of chemical solution.

NanoDSF. Proteins were diluted in PBS (100 mM Phosphate, pH 6.8, 150 mM NaCl) to a concentration of ~10 µM. Ligands were tested at a concentration of 200 µM. The intrinsic fluorescence signal was measured as a function of increasing temperature with a Prometheus NT.48 fluorimeter (NanoTemper Technologies), with 55% excitation light intensity and 1 °C/min temperature ramp. Analyses were done on capillaries filled with 10 µL of the respective samples. Intrinsic fluorescence signals expressed by the 350 nm/330 nm emission ratio that increases as the proteins unfold, were plotted as a function of temperature (Figure 5**A** and Figure 5**B**). The plots show one of the three independent data collections performed for each protein.

Intrinsic tryptophan fluorescence assays and determination of the dissociation constant K_D. These experiments were performed as described previously in de Saint Germain et al.[61] using a Spark Multimode Microplate Reader (Tecan).

Hydrolysis of (±)-SdL19 and (±)-GR24 in aqueous solution. (±)-GR24 and (±)-SdL19 were tested for their

chemical stability in an aqueous solution. Aqueous solutions of the compound to be tested (50 µg/mL) were incubated at 22 °C in the HPLC vials. The compounds were first dissolved in DMSO (2 mg/mL). Then, 25 µL of these solutions ((±)-GR24 and (±)-SdL19) were diluted to the final concentration with H_2O (750 µL) and EtOH (175 µL) and the solution adjusted to pH 6.8. Aqueous solutions of the compounds to be tested (50 µg/mL) were incubated at 22 °C in the HPLC vials. (±)-1-Indanol (25 µL of a 1 mg/mL solution in DMSO) was added as internal standard to each solution. The samples were subjected to reverse-phase-ultra-performance liquid chromatography (RP-UPLC)-MS analyses by means of UPLC system equipped with a Photo Diode Array (PDA) and a Triple Quadrupole Detector (TQD) mass spectrometer (Acquity UPLC-TQD, Waters). RP-UPLC (HSS C_{18} column, 1.8 µm, 2.1 mm × 50 mm) with 0.1% (v/v) formic acid in CH_3CN and 0.1% (v/v) formic acid in water (aq. FA, 0.1%, v/v, pH 2.8) as eluents [10% CH_3CN, followed by linear gradient from 10% to 100% of CH_3CN (4 min)] at a flow rate of 0.6 mL.min^{-1}. The detection was done by PDA and with the TQD mass spectrometer operated in Electrospray ionization-positive mode at 3.2 kV capillary voltage. To maximize the signal, the cone voltage and collision energy were optimized to 20 V and 12 eV, respectively. The collision gas was argon at a pressure maintained near 4.5 10^{-3} mBar. The relative quantity of remaining (non degraded) product was determined by integration in comparison with the internal standard.

Statistical analyses. Because deviations from normality were observed for axillary bud length after SL treatment, the Kruskal–Wallis test was used to compare treatments using R Commander version 1.7–3[88]. For bioassays with *Arabidopsis thaliana*, data were analyzed with the Shapiro-Wilkinson normality test. For bioassays with AM fungi, data were analyzed using Statgraphics Centurion software (SigmaPlus). Non-parametric tests were used because normality or homoscedasticity criteria were not met. Datasets were analyzed using the Kruskal-Wallis test, followed by pairwise comparisons with Mann-Whitney U test.

ASSOCIATED CONTENT

The Supporting Information is available free of charge at https://pubs.acs.org/doi/xxx. Crystallographic data of racemic SdL50 (Table S1) and CIF file, bioactivity data (supplementary data for Figure 7, Tables S2-S3, Figure S1) and ^{1}H and ^{13}C NMR spectra for the SdL compounds and precursors (**21; 22a,b**; **23a,b**).

AUTHOR INFORMATION

Corresponding Author

François-Didier Boyer – Université Paris-Saclay, CNRS, Institut de Chimie des Substances Naturelles, UPR 2301, 91198, Gif-sur-Yvette, France; orcid.org/0000-0001-9855-7234; tel, ++33-1-69823017; Email francois-didier.boyer@cnrs.fr

Authors

Suzanne Daignan Fornier – Université Paris-Saclay, CNRS, Institut de Chimie des Substances Naturelles, UPR 2301, 91198, Gif-sur-Yvette, France; suzanne.daignan@cnrs.fr

Alexandre de Saint Germain – Université Paris-Saclay, INRAE, AgroParisTech, Institut Jean-Pierre Bourgin (IJPB), 78000, Versailles, France; Alexandre.De-Saint-Germain@inrae.fr; orcid.org/0000-0003-2814-7234

Pascal Retailleau – Université Paris-Saclay, CNRS, Institut de Chimie des Substances Naturelles, UPR 2301, 91198, Gif-sur-Yvette, France; pascal.retailleau@cnrs.fr; orcid.org/0000-0003-3995-519X

Jean-Paul Pillot – Université Paris-Saclay, INRAE, AgroParisTech, Institut Jean-Pierre Bourgin (IJPB), 78000, Versailles, France; jean-paul.pillot@inrae.fr

Quentin Taulera – Laboratoire de Recherche en Sciences Végétales, Université de Toulouse, CNRS, UPS, Toulouse INP, 31320 Auzeville-Tolosane, France; quentin.taulera@lrsv.ups-tlse.fr

Lucile Andna – Université de Strasbourg, Institut de Chimie, UMR 7177, Équipe Synthèse Organique et Phytochimie, 4 rue Blaise Pascal CS 90032, 67081 Strasbourg Cedex France; ljouffro@its.jnj.com; orcid.org/0000-0002-4185-9458

Laurence Miesch – Université de Strasbourg, Institut de Chimie, UMR 7177, Équipe Synthèse Organique et Phytochimie, 4 rue Blaise Pascal CS 90032, 67081 Strasbourg Cedex France; lmiesch@unistra.fr; orcid.org/0000-0002-0369-9908

Soizic Rochange – Laboratoire de Recherche en Sciences Végétales, Université de Toulouse, CNRS, UPS, Toulouse INP, 31320 Auzeville-Tolosane, France; rochange@lrsv.ups-tlse.fr; orcid.org/0000-0002-3889-7859

Jean-Bernard Pouvreau – Nantes Université, CNRS, US2BN, UMR 6286, F-44000 Nantes, France; Jean-Bernard.Pouvreau@univ-nantes.fr; orcid.org/0000-0002-8351-9195

Author Contributions

F.-D.B. designed research; F.-D.B and S.D.F. designed and synthesized the SdL analogs; L.A. and L.M. synthesized (±)-MeCLA; F.-D.B. performed the HPLC analyses; F.-D.B., J.-B.P., J.-P.P., S.R. and Q.T. designed and performed the biological experiments; A.deS.G. performed the biochemical experiments. P.R. performed the X-ray analysis. All authors analyzed the data; S.R. and F.-D.B. wrote the paper. All authors critically revised the manuscript and approved the submitted version.

Funding Sources

We are grateful to Hemp *it adn* for financial support. The IJPB benefits from the support of Saclay Plant Sciences-SPS (ANR-17-EUR-0007). This work has benefited from the support of IJPB's Plant Observatory technological platforms. A.d.S.G. has received the support of the EU in the framework of the Marie-Curie FP7 COFUND People Programme, through the award of an AgreenSkills/AgreenSkills+ fellowship and the support of Saclay Plant Sciences-SPS (ANR-17-EUR-0007) through the award of a fellowship. The work of S.R. and Q.T. was supported by the TULIP LabEx (ANR-10-LABX-41). The CHARM3AT LabEx program (ANR-11-LABX-39) is also acknowledged for its support.

Notes

The authors declare no competing financial interest.

ACKNOWLEDGMENT

The authors thank Catherine Rameau for statistical analyses and Adrian Scaffidi for the generous gift of a sample of (±)-carlactone. The authors thank Jean-Marie Beau, Catherine

Rameau and Sandrine Bonhomme for comments on the manuscript.

REFERENCES

1 Cook, C. E., Whichard, L. P., Turner, B. & Wall, M. E. Germination of Witchweed (Striga Lutea Lour) - Isolation and Properties of a Potent Stimulant. *Science* **154**, 1189-1190, doi:10.1126/science.154.3753.1189 (1966).

2 Gomez-Roldan, V., Fermas, S., Brewer, P. B., Puech-Pages, V., Dun, E. A., Pillot, J.-P., Letisse, F., Matusova, R., Danoun, S., Portais, J.-C., Bouwmeester, H., Bécard, G., Beveridge, C. A., Rameau, C. & Rochange, S. F. Strigolactone inhibition of shoot branching. *Nature* **455**, 189-194, doi:10.1038/nature07271 (2008).

3 Umehara, M., Hanada, A., Yoshida, S., Akiyama, K., Arite, T., Takeda-Kamiya, N., Magome, H., Kamiya, Y., Shirasu, K., Yoneyama, K., Kyozuka, J. & Yamaguchi, S. Inhibition of shoot branching by new terpenoid plant hormones. *Nature* **455**, 195-200, doi:10.1038/nature07272 (2008).

4 Waters, M. T., Gutjahr, C., Bennett, T. & Nelson, D. C. Strigolactone Signaling and Evolution. *Annu. Rev. Plant Biol.* **68**, 291-322, doi:10.1146/annurev-arplant-042916-040925 (2017).

5 Lopez-Obando, M., Ligerot, Y., Bonhomme, S., Boyer, F.-D. & Rameau, C. Strigolactone biosynthesis and signaling in plant development. *Development* **142**, 3615-3619, doi:10.1242/dev.120006 (2015).

6 Yoneyama, K., Xie, X., Yoneyama, K., Kisugi, T., Nomura, T., Nakatani, Y., Akiyama, K. & McErlean, C. S. P. Which are the major players, canonical or non-canonical strigolactones? *J. Exp. Bot.* **69**, 2231-2239, doi:10.1093/jxb/ery090 (2018).

7 Wakabayashi, T., Hamana, M., Mori, A., Akiyama, R., Ueno, K., Osakabe, K., Osakabe, Y., Suzuki, H., Takikawa, H., Mizutani, M. & Sugimoto, Y. Direct conversion of carlactonoic acid to orobanchol by cytochrome P450 CYP722C in strigolactone biosynthesis. *Sci. Adv.* **5**, eaax9067, doi:10.1126/sciadv.aax9067 (2019).

8 Wakabayashi, T., Shida, K., Kitano, Y., Takikawa, H., Mizutani, M. & Sugimoto, Y. CYP722C from *Gossypium arboreum* catalyzes the conversion of carlactonoic acid to 5-deoxystrigol. *Planta* **251**, 97, doi:10.1007/s00425-020-03390-6 (2020).

9 Mori, N., Sado, A., Xie, X., Yoneyama, K., Asami, K., Seto, Y., Nomura, T., Yamaguchi, S., Yoneyama, K. & Akiyama, K. Chemical identification of 18-hydroxycarlactonoic acid as an LjMAX1 product and *in planta* conversion of its methyl ester to canonical and non-canonical strigolactones in Lotus japonicus. *Phytochemistry* **174**, 112349, doi:10.1016/j.phytochem.2020.112349 (2020).

10 Wang, J. Y., Lin, P.-Y. & Al-Babili, S. On the biosynthesis and evolution of apocarotenoid plant growth regulators. *Seminars in Cell & Developmental Biology* **109**, 3-11, doi:10.1016/j.semcdb.2020.07.007 (2021).

11 Yoda, A., Mori, N., Akiyama, K., Kikuchi, M., Xie, X., Miura, K., Yoneyama, K., Sato-Izawa, K., Yamaguchi, S., Yoneyama, K., Nelson, D. C. & Nomura, T. Strigolactone biosynthesis catalyzed by cytochrome P450 and sulfotransferase in sorghum. *New Phytol.* **232**, 1999-2010, doi:10.1111/nph.17737 (2021).

12 Brewer, P. B., Yoneyama, K., Filardo, F., Meyers, E., Scaffidi, A., Frickey, T., Akiyama, K., Seto, Y., Dun, E. A., Cremer, J. E., Kerr, S. C., Waters, M. T., Flematti, G. R., Mason, M. G., Weiller, G., Yamaguchi, S., Nomura, T., Smith, S. M. & Beveridge, C. A. LATERAL BRANCHING OXIDOREDUCTASE acts in the final stages of strigolactone biosynthesis in Arabidopsis. *Proc. Natl. Acad. Sci. U.S.A.* **113**, 6301-6306, doi:10.1073/pnas.1601729113 (2016).

13 Yoneyama, K., Akiyama, K., Brewer, P. B., Mori, N., Kawano-Kawada, M., Haruta, S., Nishiwaki, H., Yamauchi, S., Xie, X., Umehara, M., Beveridge, C. A., Yoneyama, K. & Nomura, T. Hydroxyl carlactone derivatives are predominant strigolactones in *Arabidopsis*. *Plant Direct* **4**, e00219, doi:10.1002/pld3.219 (2020).

14 Yoneyama, K. Recent progress in the chemistry and biochemistry of strigolactones. *J. Pestic. Sci.* **45**, 45-53, doi:10.1584/jpestics.D19-084 (2020).

15 Bromhead, L. J. & McErlean, C. S. P. Accessing Single Enantiomer Strigolactones: Progress and Opportunities. *Eur. J. Org. Chem.*, 5712-5723, doi:10.1002/ejoc.201700865 (2017).

16 Yasui, M., Ota, R., Tsukano, C. & Takemoto, Y. Total synthesis of avenaol. *Nat. Commun.* **8**, 674, doi:10.1038/s41467-017-00792-1 (2017).

17 Yasui, M., Yamada, A., Tsukano, C., Hamza, A., Pápai, I. & Takemoto, Y. Enantioselective Acetalization by Dynamic Kinetic Resolution for the Synthesis of γ-Alkoxybutenolides by Thiourea/Quaternary Ammonium Salt Catalysts: Application to Strigolactones. *Angew. Chem. Int. Ed.* **59**, 13479-13483, doi:10.1002/anie.202002129 (2020).

18 Yoshimura, M., Dieckmann, M., Dakas, P.-Y., Fonné-Pfister, R., Screpanti, C., Hermann, K., Rendine, S., Quinodoz, P., Horoz, B., Catak, S. & De Mesmaeker, A. Total Synthesis and Biological Evaluation of Zealactone 1a/b. *Helv. Chim. Acta* **103**, e2000017, doi:10.1002/hlca.202000017 (2020).

19 Takahashi, I. & Asami, T. Target-based selectivity of strigolactone agonists and antagonists in plants and their potential use in agriculture. *J. Exp. Bot.* **69**, 2241-2254, doi:10.1093/jxb/ery126 (2018).

20 Jamil, M., Kountche, B. A. & Al-Babili, S. Current progress in *Striga* management. *Plant Physiol.* **185**, 1339-1352, doi:10.1093/plphys/kiab040 (2021).

21 Johnson, A. W., Gowda, G., Hassanali, A., Knox, J., Monaco, S., Razavi, Z. & Rosebery, G. The Preparation of Synthetic Analogs of Strigol. *J. Chem. Soc., Perkin Trans. 1*, 1734-1743, doi:10.1039/P19810001734 (1981).

22 Kodama, K., Rich, M. K., Yoda, A., Shimazaki, S., Xie, X., Akiyama, K., Mizuno, Y., Komatsu, A., Luo, Y., Suzuki, H., Kameoka, H., Libourel, C., Keller, J., Sakakibara, K., Nishiyama, T., Nakagawa, T., Mashiguchi, K., Uchida, K., Yoneyama, K., Tanaka, Y., Yamaguchi, S., Shimamura, M., Delaux, P.-M., Nomura, T. & Kyozuka, J. An Ancestral Function of Strigolactones as Symbiotic Rhizosphere Signals. *bioRxiv*, doi:10.1101/2021.08.20.457034 (2021).

23 Boyer, F.-D., de Saint Germain, A., Pillot, J.-P., Pouvreau, J.-B., Chen, V. X., Ramos, S., Stévenin, A., Simier, P., Delavault, P., Beau, J.-M. & Rameau, C. Structure-Activity Relationship Studies of Strigolactone-Related Molecules for Branching Inhibition in Garden Pea: Molecule Design for Shoot Branching. *Plant Physiol.* **159**, 1524-1544, doi:10.1104/pp.112.195826 (2012).

24 Umehara, M., Cao, M., Akiyama, K., Akatsu, T., Seto, Y., Hanada, A., Li, W., Takeda-Kamiya, N., Morimoto, Y. & Yamaguchi, S. Structural Requirements of Strigolactones for Shoot Branching Inhibition in Rice and *Arabidopsis*. *Plant Cell Physiol.* **56**, 1059-1072, doi:10.1093/pcp/pcv028 (2015).

25 Xie, X., Yoneyama, K. & Yoneyama, K. The Strigolactone Story. *Annu. Rev. Phytopathol.* **48**, 93-117, doi:10.1146/annurev-phyto-073009-114453 (2010).

26 Mori, N., Nishiuma, K., Sugiyama, T., Hayashi, H. & Akiyama, K. Carlactone-type strigolactones and their synthetic analogues as inducers of hyphal branching in arbuscular mycorrhizal fungi. *Phytochemistry* **130**, 90-98, doi:10.1016/j.phytochem.2016.05.012 (2016).

27 Jamil, M., Kountche, B. A., Wang, J. Y., Haider, I., Jia, K. P., Takahashi, I., Ota, T., Asami, T. & Al-Babili, S. A New Series of Carlactonoic Acid Based Strigolactone Analogs for Fundamental and Applied Research. *Front. Plant Sci.* **11**, 434, doi:10.3389/fpls.2020.00434 (2020).

28 Jamil, M., Kountche, B. A., Haider, I., Guo, X., Ntui, V. O., Jia, K.-P., Ali, S., Hameed, U. S., Nakamura, H., Lyu, Y., Jiang, K., Hirabayashi, K., Tanokura, M., Arold, S. T., Asami, T. & Al-Babili, S. Methyl phenlactonoates are efficient

strigolactone analogs with simple structure. *J. Exp. Bot.* **69**, 2319-2331, doi:10.1093/jxb/erx438 (2018).

29 Parker, C. Parasitic Weeds: A World Challenge. *Weed Sci.* **60**, 269-276, doi:10.1614/WS-D-11-00068.1 (2012).

30 Grenz, J. H. & Sauerborn, J. Mechanisms limiting the geographical range of the parasitic weed *Orobanche crenata*. *Agric. Ecosyst. Environ.* **122**, 275-281, doi:10.1016/j.agee.2007.01.014 (2007).

31 Delavault, P., Montiel, G., Brun, G., Pouvreau, J. B., Thoiron, S. & Simier, P. Communication Between Host Plants and Parasitic Plants. *Adv. Bot. Res.* **82**, 55-82, doi:10.1016/bs.abr.2016.10.006 (2017).

32 Brun, G., Spallek, T., Simier, P. & Delavault, P. Molecular actors of seed germination and haustoriogenesis in parasitic weeds. *Plant Physiol.* **185**, 1270-1281, doi:10.1093/plphys/kiaa041 (2021).

33 Fernandez-Aparicio, M., Reboud, X. & Gibot-Leclerc, S. Broomrape Weeds. Underground Mechanisms of Parasitism and Associated Strategies for their Control: A Review. *Front. Plant Sci.* **7**, 135, doi:10.3389/fpls.2016.00135 (2016).

34 Akiyama, K., Matsuzaki, K. & Hayashi, H. Plant sesquiterpenes induce hyphal branching in arbuscular mycorrhizal fungi. *Nature* **435**, 824-827, doi:10.1038/nature03608 (2005).

35 Besserer, A., Puech-Pages, V., Kiefer, P., Gomez-Roldan, V., Jauneau, A., Roy, S., Portais, J. C., Roux, C., Bécard, G. & Sejalon-Delmas, N. Strigolactones stimulate arbuscular mycorrhizal fungi by activating mitochondria. *PLoS Biol.* **4**, 1239-1247, doi:e226 (2006).

36 Besserer, A., Bécard, G., Jauneau, A., Roux, C. & Sejalon-Delmas, N. GR24, a synthetic analog of strigolactones, stimulates the mitosis and growth of the arbuscular mycorrhizal fungus *Gigaspora rosea* by boosting its energy metabolism. *Plant Physiol.* **148**, 402-413, doi:10.1104/pp.108.121400 (2008).

37 Rich, M. K., Vigneron, N., Libourel, C., Keller, J., Xue, L., Hajheidari, M., Radhakrishnan Guru, V., Le Ru, A., Diop Seydina, I., Potente, G., Conti, E., Duijsings, D., Batut, A., Le Faouder, P., Kodama, K., Kyozuka, J., Sallet, E., Bécard, G., Rodriguez-Franco, M., Ott, T., Bertrand-Michel, J., Oldroyd Giles, E. D., Szövényi, P., Bucher, M. & Delaux, P.-M. Lipid exchanges drove the evolution of mutualism during plant terrestrialization. *Science* **372**, 864-868, doi:10.1126/science.abg0929 (2021).

38 Stojanova, B., Delourme, R., Duffé, P., Delavault, P. & Simier, P. Genetic differentiation and host preference reveal non-exclusive host races in the generalist parasitic weed Phelipanche ramosa. *Weed Res.* **59**, 107-118, doi:10.1111/wre.12353 (2019).

39 Huet, S., Pouvreau, J.-B., Delage, E., Delgrange, S., Marais, C., Bahut, M., Delavault, P., Simier, P. & Poulin, L. Populations of the Parasitic Plant *Phelipanche ramosa* Influence Their Seed Microbiota. *Front. Plant Sci.* **11**, 1075, doi:10.3389/fpls.2020.01075 (2020).

40 Auger, B., Pouvreau, J.-B., Pouponneau, K., Yoneyama, K., Montiel, G., Le Bizec, B., Yoneyama, K., Delavault, P., Delourme, R. & Simier, P. Germination Stimulants of *Phelipanche ramosa* in the Rhizosphere of *Brassica napus* Are Derived from the Glucosinolate Pathway. *Mol. Plant-Microbe Interact.* **25**, 993-1004, doi:10.1094/mpmi-01-12-0006-r (2012).

41 Xie, X., Kusumoto, D., Takeuchi, Y., Yoneyama, K., Yamada, Y. & Yoneyama, K. 2 '-Epi-orobanchol and solanacol, two unique strigolactones, germination stimulants for root parasitic weeds, produced by tobacco. *J. Agric. Food. Chem.* **55**, 8067-8072, doi:10.1021/jf0715121 (2007).

42 Xie, X., Yoneyama, K., Kisugi, T., Uchida, K., Ito, S., Akiyama, K., Hayashi, H., Yokota, T., Nomura, T. & Yoneyama, K. Confirming Stereochemical Structures of Strigolactones Produced by Rice and Tobacco. *Mol. Plant* **6**, 153-163, doi:10.1093/mp/sss139 (2013).

43 Koltai, H., Cohen, M., Chesin, O., Mayzlish-Gati, E., Bécard, G., Puech, V., Ben Dor, B., Resnick, N., Wininger, S. & Kapulnik, Y. Light is a positive regulator of strigolactone levels in tomato roots. *J. Plant Physiol.* **168**, 1993-1996, doi:10.1016/j.jplph.2011.05.022 (2011).

44 Hamzaoui, O., Maciuk, A., Delgrange, S., Kerdja, K., Thouminot, C., Germain, A. d. S., Rochange, S., Boyer, F.-D., Simier, P. & Pouvreau, J.-B. Cannalactone: a new non-canonical strigolactone exudated by *Cannabis sativa* roots with a pivotal role in host specialization within French broomrape (*Phelipanche ramosa*) populations in *15th World Congress on Parasitic Plants*. (Amsterdam, 2019).

45 de Saint Germain, A., Retailleau, P., Norsikian, S., Servajean, V., Pelissier, F., Steinmetz, V., Pillot, J.-P., Rochange, S., Pouvreau, J.-B. & Boyer, F.-D. Contalactone, a contaminant formed during chemical synthesis of the strigolactone reference GR24 is also a strigolactone mimic. *Phytochemistry* **168**, 112112, doi:10.1016/j.phytochem.2019.112112 (2019).

46 Hamiaux, C., Drummond, R. S. M., Janssen, B. J., Ledger, S. E., Cooney, J. M., Newcomb, R. D. & Snowden, K. C. DAD2 Is an α/β Hydrolase Likely to Be Involved in the Perception of the Plant Branching Hormone, Strigolactone. *Curr. Biol.* **22**, 2032-2036, doi:10.1016/j.cub.2012.08.007 (2012).

47 Waters, M. T., Nelson, D. C., Scaffidi, A., Flematti, G. R., Sun, Y. K., Dixon, K. W. & Smith, S. M. Specialisation within the DWARF14 protein family confers distinct responses to karrikins and strigolactones in *Arabidopsis*. *Development* **139**, 1285-1295, doi:10.1242/dev.074567 (2012).

48 Conn, C. E., Bythell-Douglas, R., Neumann, D., Yoshida, S., Whittington, B., Westwood, J. H., Shirasu, K., Bond, C. S., Dyer, K. A. & Nelson, D. C. Convergent evolution of strigolactone perception enabled host detection in parasitic plants. *Science* **349**, 540-543, doi:10.1126/science.aab1140 (2015).

49 Toh, S., Holbrook-Smith, D., Stogios, P. J., Onopriyenko, O., Lumba, S., Tsuchiya, Y., Savchenko, A. & McCourt, P. Structure-function analysis identifies highly sensitive strigolactone receptors in *Striga*. *Science* **350**, 203-207, doi:10.1126/science.aac9476 (2015).

50 Nelson, D. C. The mechanism of host-induced germination in root parasitic plants. *Plant Physiol.* **185**, 1353-1373, doi:10.1093/plphys/kiab043 (2021).

51 de Saint Germain, A., Jacobs, A., Brun, G., Pouvreau, J.-B., Braem, L., Cornu, D., Clavé, G., Baudu, E., Steinmetz, V., Servajean, V., Wicke, S., Gevaert, K., Simier, P., Goormachtig, S., Delavault, P. & Boyer, F.-D. A *Phelipanche ramosa* KAI2 protein perceives strigolactones and isothiocyanates enzymatically. *Plant Commun.* **2**, 100166, doi:10.1016/j.xplc.2021.100166 (2021).

52 Križková, P. M., Lindner, W. & Hammerschmidt, F. Improved Synthesis of Racemate and Enantiomers of Taniguchi Lactone and Conversion of Their C-C Double Bonds into Triple Bonds. *Synthesis* **50**, 651-657, doi:10.1055/s-0036-1591516 (2018).

53 Ballini, R., Marcantoni, E. & Perella, S. A Two Steps Synthesis of γ-Substituted and γ,γ-Disubstituted α-(Alkylmethylene)-γ-butyrolactones. *J. Org. Chem.* **64**, 2954-2957, doi:10.1021/jo982131c (1999).

54 Bartoli, G., Marcantoni, E. & Petrini, M. CeCl3-Mediated Addition of Grignard Reagents to 1,3-Diketones. *Angew. Chem. Int. Ed.* **32**, 1061-1062, doi:10.1002/anie.199310611 (1993).

55 Oriyama, T., Kobayashi, Y. & Noda, K. Chemoselective and Practical Deprotection of Alkyl Trialkylsilyl Ethers in the Presence of Aryl Trialkylsilyl Ethers by a Catalytic Amount of Sc(OTf)3. *Synlett*, 1047-1048, doi:10.1055/s-1998-1890 (1998).

56 Norsikian, S., Holmes, I., Lagasse, F. & Kagan, H. B. A one-pot esterification of chiral *O*-trimethylsilyl-cyanohydrins with retention of stereochemistry. *Tetrahedron Lett.* **43**, 5715-5717, doi:10.1016/S0040-4039(02)01200-5 (2002).

57 Pouvreau, J. B., Gaudin, Z., Auger, B., Lechat, M. M., Gauthier, M., Delavault, P. & Simier, P. A high-throughput

seed germination assay for root parasitic plants. *Plant Methods* **9**, 32, doi:10.1186/1746-4811-9-32 (2013).

58 Miura, H., Ochi, R., Nishiwaki, H., Yamauchi, S., Xie, X., Nakamura, H., Yoneyama, K. & Yoneyama, K. Germination Stimulant Activity of Isothiocyanates on *Phelipanche* spp. *Plants* **11**, 606, doi:10.3390/plants11050606 (2022).

59 Boyer, F.-D., de Saint Germain, A., Pillot, J. P., Pouvreau, J.-B., Chen, V. X., Ramos, S., Stevenin, A., Simier, P., Delavault, P., Beau, J.-M. & Rameau, C. Structure-activity relationship studies of strigolactone-related molecules for branching inhibition in garden pea: molecule design for shoot branching. *Plant Physiol.* **159**, 1524-1544, doi:10.1104/pp.112.195826 (2012).

60 Boyer, F.-D., de Saint Germain, A., Pouvreau, J.-B., Clavé, G., Pillot, J.-P., Roux, A., Rasmussen, A., Depuydt, S., Lauressergues, D., Frei dit Frey, N., Heugebaert, T. S. A., Stevens, C. V., Geelen, D., Goormachtig, S. & Rameau, C. New Strigolactone Analogs as Plant Hormones with Low Activities in the Rhizosphere. *Mol. Plant* **7**, 675-690, doi:10.1093/mp/sst163 (2014).

61 de Saint Germain, A., Clavé, G., Badet-Denisot, M.-A., Pillot, J.-P., Cornu, D., Le Caer, J.-P., Burger, M., Pelissier, F., Retailleau, P., Turnbull, C., Bonhomme, S., Chory, J., Rameau, C. & Boyer, F.-D. An histidine covalent receptor and butenolide complex mediates strigolactone perception. *Nat. Chem. Biol.* **12**, 787-794, doi:10.1038/nchembio.2147 (2016).

62 Auldridge, M. E., Block, A., Vogel, J. T., Dabney-Smith, C., Mila, I., Bouzayen, M., Magallanes-Lundback, M., DellaPenna, D., McCarty, D. R. & Klee, H. J. Characterization of three members of the Arabidopsis carotenoid cleavage dioxygenase family demonstrates the divergent roles of this multifunctional enzyme family. *Plant J.* **45**, 982-993, doi:10.1111/j.1365-313X.2006.02666.x (2006).

63 Xie, X. Structural diversity of strigolactones and their distribution in the plant kingdom. *J. Pestic. Sci.* **41**, 175-180, doi:10.1584/jpestics.J16-02 (2016).

64 Akiyama, K., Ogasawara, S., Ito, S. & Hayashi, H. Structural Requirements of Strigolactones for Hyphal Branching in AM Fungi. *Plant Cell Physiol.* **51**, 1104-1117, doi:10.1093/pcp/pcq058 (2010).

65 Taulera, Q., Lauressergues, D., Martin, K., Cadoret, M., Servajean, V., Boyer, F.-D. & Rochange, S. Initiation of arbuscular mycorrhizal symbiosis involves a novel pathway independent from hyphal branching. *Mycorrhiza* **30**, 491-501, doi:10.1007/s00572-020-00965-9 (2020).

66 López-Ráez, J. A., Charnikhova, T., Gomez-Roldan, V., Matusova, R., Kohlen, W., De Vos, R., Verstappen, F., Puech-Pages, V., Becard, G., Mulder, P. & Bouwmeester, H. Tomato strigolactones are derived from carotenoids and their biosynthesis is promoted by phosphate starvation. *New Phytol.* **178**, 863-874 (2008).

67 Decker, E. L., Alder, A., Hunn, S., Ferguson, J., Lehtonen, M. T., Scheler, B., Kerres, K. L., Wiedemann, G., Safavi-Rizi, V., Nordzieke, S., Balakrishna, A., Baz, L., Avalos, J., Valkonen, J. P. T., Reski, R. & Al-Babili, S. Strigolactone biosynthesis is evolutionarily conserved, regulated by phosphate starvation and contributes to resistance against phytopathogenic fungi in a moss, *Physcomitrella patens*. *New Phytol.* **216**, 455-468, doi:10.1111/nph.14506 (2017).

68 Lopez-Obando, M., Guillory, A., Boyer, F.-D., Cornu, D., Hoffmann, B., Le Bris, P., Pouvreau, J.-B., Delavault, P., Rameau, C., de Saint Germain, A. & Bonhomme, S. The *Physcomitrium (Physcomitrella*) patens PpKAI2L receptors for strigolactones and related compounds function via MAX2-dependent and -independent pathways. *Plant Cell* **33**, 3487-3512, doi:10.1093/plcell/koab217 (2021).

69 Mangnus, E. M., Dommerholt, F. J., Dejong, R. L. P. & Zwanenburg, B. Improved Synthesis of Strigol Analog GR24 and Evaluation of the Biological-Activity of Its Diastereomers. *J. Agric. Food. Chem.* **40**, 1230-1235, doi:10.1021/jf00019a031 (1992).

70 Scaffidi, A., Waters, M. T., Ghisalberti, E. L., Dixon, K. W., Flematti, G. R. & Smith, S. M. Carlactone-independent seedling morphogenesis in Arabidopsis. *Plant J.* **76**, 1-9, doi:10.1111/tpj.12265 (2013).

71 Boutet-Mercey, S., Perreau, F., Roux, A., Clavé, G., Pillot, J.-P., Schmitz-Afonso, I., Touboul, D., Mouille, G., Rameau, C. & Boyer, F.-D. Validated Method for Strigolactone Quantification by Ultra High-Performance Liquid Chromatography – Electrospray Ionisation Tandem Mass Spectrometry Using Novel Deuterium Labelled Standards. *Phytochem. Anal.* **29**, 59-68, doi:10.1002/pca.2714 (2018).

72 Chen, V. X., Boyer, F.-D., Rameau, C., Pillot, J.-P., Vors, J.-P. & Beau, J.-M. New Synthesis of A-Ring Aromatic Strigolactone Analogues and Their Evaluation as Plant Hormones in Pea (*Pisum sativum*). *Chem. – Eur. J.* **19**, 4849-4857, doi:10.1002/chem.201203585 (2013).

73 Macalpine, G. A., Raphael, R. A., Shaw, A., Taylor, A. W. & Wild, H. J. Synthesis of Germination Stimulant (±)-Strigol. *J. Chem. Soc., Perkin Trans. 1*, 410-416, doi:10.1039/C39740000834 (1976).

74 Sugano, G., Kawada, K., Shigeta, M., Hata, T. & Urabe, H. Iron-catalyzed δ-selective conjugate addition of methyl and cyclopropyl Grignard reagents to α,β,γ,δ-unsaturated esters and amides. *Tetrahedron Lett.* **60**, 885-890, doi:10.1016/j.tetlet.2018.12.043 (2019).

75 Rigaku, O. D. CrystalClear-SM Expert 2.0 r4 Rigaku Corporation, Tokyo, Japan. (2009).

76 Schneider, T. R. & Sheldrick, G. M. Substructure solution with SHELXD. *Acta Crystallogr., Sect. D: Biol. Crystallogr.* **58**, 1772-1779, doi:doi:10.1107/S0907444902011678 (2002).

77 Sheldrick, G. M. Crystal structure refinement with SHELXL. *Acta Crystallogr., Sect. C: Cryst. Struct. Commun.* **71**, 3-8, doi:10.1107/s2053229614024218 (2015).

78 Sheldrick, G. M. SHELXT - Integrated space-group and crystal-structure determination. *Acta Crystallogr., Sect. A: Found. Crystallogr.* **71**, 3-8, doi:10.1107/s2053273314026370 (2015).

79 Spek, A. L. Structure validation in chemical crystallography. *Acta Crystallogr., Sect. D: Biol. Crystallogr.* **65**, 148-155, doi:10.1107/s090744490804362x (2009).

80 Spek, A. L. PLATONSQUEEZE: a tool for the calculation of the disordered solvent contribution to the calculated structure factors. *Acta Crystallogr., Sect. C: Cryst. Struct. Commun.* **71**, 9-18, doi:10.1107/s2053229614024929 (2015).

81 Rameau, C., Bodelin C, Cadier D, Grandjean O, Miard F & Murfet IC. New *ramosus* mutants at loci *Rms1*, *Rms3* and *Rms4* resulting from the mutation breeding program at Versailles. *Pisum Genetics* **29**, 7-12 (1997).

82 Braun, N., de Saint Germain, A., Pillot, J. P., Boutet-Mercey, S., Dalmais, M., Antoniadi, I., Li, X., Maia-Grondard, A., Le Signor, C., Bouteiller, N., Luo, D., Bendahmane, A., Turnbull, C. & Rameau, C. The pea TCP transcription factor PsBRC1 acts downstream of Strigolactones to control shoot branching. *Plant Physiol.* **158**, 225-238, doi:10.1104/pp.111.182725 (2012).

83 Cornet, F., Pillot, J.-P., Le Bris, P., Pouvreau, J.-B., Arnaud, N., de Saint Germain, A. & Rameau, C. Strigolactones (SLs) modulate the plastochron by regulating KLUH (KLU) transcript abundance in Arabidopsis. *New Phytol.* **232**, 1909-1916, doi:10.1111/nph.17725 (2021).

84 Muñoz, A., Pillot, J.-P., Cubas, P. & Rameau, C. Methods for Phenotyping Shoot Branching and Testing Strigolactone Bioactivity for Shoot Branching in Arabidopsis and Pea in *Strigolactones: Methods and Protocols* (eds Cristina Prandi & Francesca Cardinale) 115-127 (Springer US, 2021). doi:10.1007/978-1-0716-1429-7_10.

85 Pouvreau, J.-B., Poulin, L., Huet, S. & Delavault, P. Strigolactone-Like Bioactivity via Parasitic Plant Germination Bioassay in *Strigolactones: Methods and Protocols* (eds Cristina Prandi & Francesca Cardinale) 59-73 (Springer US, 2021). doi:10.1007/978-1-0716-1429-7_6.

86 Bécard, G. & Fortin, J. A. Early events of vesicular arbuscular mycorrhiza formation on Ri T-DNA transformed roots. *New Phytol.* **108**, 211-218, doi:10.1111/j.1469-8137.1988.tb03698.x (1988).

87 Lauressergues, D., André, O., Peng, J., Wen, J., Chen, R., Ratet, P., Tadege, M., Mysore, K. S. & Rochange, S. F. Strigolactones contribute to shoot elongation and to the formation of leaf margin serrations in *Medicago truncatula* R108. *J. Exp. Bot.* **66**, 1237-1244, doi:10.1093/jxb/eru471 (2015).

88 Fox, J. The R commander: A basic-statistics graphical user interface to R. *J. Stat. Softw.* **14**, 1-42, doi:10.18637/jss.v014.i09 (2005).

SYNOPSIS TOC

